TK1 in Cancer Progression: elucidating its influence on cellular invasion and survival

Eliza E. Bitter
Brigham Young University
Michelle H. Townsend
Brigham Young University
Kary Y.F. Tsai
Brigham Young University
Carolyn I. Allen
Brigham Young University
Rachel I. Erickson
Brigham Young University
Brett E. Pickett
Brigham Young University
Juan A. Arroyo
Brigham Young University
Kim O'Neill (kim_oneill@byu.edu)
Brigham Young University https://orcid.org/0000-0002-8747-6217

Research article

Keywords: Thymidine Kinase 1, cell proliferation biomarker, breast cancer, cellular invasion, cell survival

Posted Date: November 20th, 2019

DOI: https://doi.org/10.21203/rs.2.17532/v1

Abstract

1. Background: The salvage pathway enzyme thymidine kinase 1 (TK1) is elevated in the serum of several different cancer types and higher expression is associated with more aggressive tumor grade. As a result, it has potential as a biomarker for diagnosis and prognosis. Recent studies indicate that TK1 may be involved in cancer pathogenesis; however, its direct involvement has not been identified. We propose to evaluate the effects of TK1 on cancer progression in vitro through measuring cellular invasion and survival of breast cancer cells.

2.Methods: Breast cancer cells MDA-MB-231, HCC 1806, and MCF7 were cultured according to standard techniques. We employed the use of TK1 target siRNA and a CRISPR-Cas9 TK1 knockout plasmid to compare transfected cell lines to wild type cell lines. Protein factors in survival and invasive pathways were also tested for correlations to TK1 in BRCA RNA-seq patient data (n=1095) using the TIMER program. Cellular invasion was quantified in cell index (factor of impedance) over a 24-hour period. Cell survival was measured by apoptosis under metabolic and DNA stress using flow cytometry. All results were statistically assessed using an ANOVA or t-test in GraphPad PRISM®.

3.Results: Cellular invasion assays assessing wild type and TK1 knockdown/knockout (TK1-/-) cell types showed TK1-/- cell lines had increased invasion potential ($p= 0.0001$). Bioinformatically, we saw a strong overall negative correlation between apoptotic factors and TK1 ($p \leq 0.05$). When testing TK1 effects on cell survival we saw a protective affect under DNA stress ($p \leq 0.05$), but not under metabolic stress ($p= 0.0001$).

4.Conclusion From cell cycle analysis, we observed a shift towards S phase in TK1-/- cells. This shift to S phase would promote growth and account for the increased cellular invasion and decrease in metabolic induced stress in TK1-/- cells. We propose that cancer cells still may elicit a cancer progressive phenotype based on effects of TK1, but that a system which isolates TK1 is not effective to understand the effects. Instead, identifying protein networks inclusive of TK1 will help to elucidate its effects on cancer progression.

Background

Following the discovery of DNA, thymidine kinase 1 was identified in regenerating rat livers (1). Later, it was identified as a protein within the DNA salvage pathway and found to be responsible for recovering thymidine prior to DNA incorporation (2). Thymidine synthesis can occur through *de novo* synthesis or the salvage pathway. *De novo* synthesis begins when deoxyuridine monophosphate (dUMP) is converted to dTMP by thymidylate synthase in the presence of folic acid and vitamin B12 (3). Further phosphorylation then takes place to form dTTP prior to DNA incorporation. While *de novo* synthesis is an effective pathway for nucleotide production, it is energetically expensive (4). As a result, the salvage pathway evolved as a mechanism of conserving energy by recovering bases and nucleosides from intermediates such as degraded RNA and DNA. It has been shown that TK1 is not essential for DNA synthesis due to the availability of the *de novo* pathway (5). Yet, TK1 is essential in certain conditions within cancer development and progression (5).

TK1 is tightly regulated at all levels of expression from mRNA transcription to protein degradation (6–10). Abnormalities in cell proliferation factors have been shown to contribute to tumor development and progression (11–13). TK1 upregulation in neoplastic cells is an early event and has been shown to be detectable in cancer patients before they manifest clinical symptoms (14). Additionally, TK1 has shown significant elevation in the serum of many different cancer types including the most commonly diagnosed cancers: lung, breast, prostate and colon (7, 8, 15–17). As a serum biomarker, the potential value of TK1 as an additional cellular proliferation marker for cancer prognosis and diagnosis has been indicated by several groups (7, 8, 15). Increased expression of the TK1 enzyme is associated with cancer aggressiveness and TK1 serum levels progressively increase with cancer grade (T1-T4) in breast tissue (14, 17)..

The role of TK1 and its impact on tumor progression has recently been evaluated in protein networks (18–20). In one study, TK1 was evaluated in invasive MDA-MB–231 cells within a protein network that included HSP90AB1, CSNK2B, YWHAB and VIM (18). Knockdowns of the complete network inhibited cellular invasion during the epithelial-mesenchymal transition when compared to non-invasive MCF7 and non-tumoral MCF–10A cell lines (18). Other studies have bioinformatically associated TK1 with additional protein networks that contribute to tumor progression in adrenocortical carcinoma (ACC) and prostate cancer (PCa) (19, 20). Alshabi et. al, identified through differentially expressed genes (DEGs) and protein-protein interaction networks in ACC patients that of all the affected pathways, pyrimidine deoxyribonucleoside salvage and cell cycle were some of the most enriched pathways (20). TK1 was found to be linked to both poor overall patient survival and increased expression in stage 4 ACC patients, which indicate TK1 correlations to tumor progression (20). Among the DEGs identified by Song et al. in PCa patients, TK1 was shown to contribute to PCa pathogenesis, increasing with stage 4 tumors (19, 20).

Although some studies have indicated TK1's potential in tumor development, understanding TK1's individual effects on cellular invasion and survival has not been identified in breast cancer. In this study, we aim to test the effect of TK1 on cellular invasion and survival by evaluating wild type and TK1 knockdown cell lines in cellular invasion and apoptotic assays. Further evaluating the role that cytosolic TK1 plays in the tumor environment is imperative to understand its potential as not just a cancer biomarker, but also as a tumor target.

Methods

1. Identifying upregulated levels of TK1 across cancer types

TK1 expression differences in normal and cancerous patients were evaluated across cancer types using the web-portal UALCAN (21). This web portal extracts RNA-seq data from TCGA for 31 different cancer types using TCGA-Assembler Software (22). Files were obtained for "Primary Solid Tissue" and for "Solid Tissue Normal" for each cancer type and the estimation of generated transcripts (scaled estimates) were converted to transcripts per million (TPM). The TPM for TK1 expression comparing normal tissue and tumor tissue are represented by box and whisker plots which depict the 25^{th} percentile, median, 75^{th} percentile and maximum values. Additionally, UALCAN provides methylation at the promoter region of specific genes within each cancer type. This was accomplished by the Infinium Methylation Assay from Illumina ®.

2. Comparing TK1 levels in metastatic and primary cancer cell lines

To distinguish differences between TK1 levels in metastatic and primary cancer cell lines, RNA-seq data was obtained through the Cancer Cell Line Encyclopedia (CCLE) (23). Cancer cell lines (n=130) were categorized as metastatic or primary based on ATCC® and Cellosaurus classification. Statistical analysis of TK1 expression was computed using Python™.

3. Immunohistochemistry of invasive ductal and infiltrating lobular tissues

When evaluating the staining intensity of breast cancer tissue for TK1, a histology slide containing adjacent normal breast, infiltrating lobular, invasive ductal, metastatic ductal and metastatic lobular was evaluated (n=96). The controls used in TK1 level analysis were GAPDH and a universal human isotype. Tissues were stained according to protocols outlined in Townsend et al. (24).

Briefly, slides were rehydrated in decreasing amounts of alcohol prior to DIVA (BioCare medical, LLC) treatment and blocked for non-specific binding. Tissues were incubated for 12-16 hours in a humidity chamber at 4°C in primary antibody, either GAPDH (Cell Signaling®, address, country; clone 14C10) or anti-TK1 (Abcam®; 1 Kendall Square, Suite B2304 Cambridge, MA 02139-1517, USA; clone 76495). The tissues were washed in TBS three times for five minutes; tissues were then treated with secondary anti-rabbit HRP (MACH 4 HRP polymer, Biocare Medical,LLC) and incubated at room temperature for 30 minutes in a humidity chamber. The tissues were washed in TBS three times for 5 minutes to remove unbound secondary. Secondary antibody conjugated to HRP was exposed to 3,3'-Diaminobenzidine (DAB), the oxidized product forms a brown precipitate. Slides were then treated with hematoxylin, washed in cold running water for 5 minutes and dehydrated in increasing amounts on alcohol before being mounted using Cystoseal^{TM} 280 (Thermo Scientific™).

Following tissue imaging, all tissues were analyzed using ImageJ software (25). Within ImageJ, tissues were evaluated for staining intensity. Images were filtered for DAB staining using 'IHC toolbox' program with a selected "more DAB" option (25) which removed areas of the sample without sufficient DAB staining. Following this, images were converted to a gray scale and then placed under a set threshold based on positive and negative controls (GAPDH and universal human isotype). The threshold 50-150 was applied to avoid bias for negative space within the image. Of note, the grayscale is inverse of staining; the lower the gray value, the darker the staining. Once the threshold was applied to all images, each image was assessed for average gray intensity. Quantified tissues were then analyzed in GraphPad PRISM® (GraphPad Software, Inc.) using a multiple comparison ANOVA test to compare TK1 levels in breast tissue type to positive and negative controls.

4. Examining TK1 correlation to cellular invasion and apoptosis in BRCA patients

The online bioinformatic tool TIMER, developed by Li T., et al (26) was used to evaluate correlations between TK1 to invasive proteins and apoptotic factors using RNA-seq BRCA patient data (n=1093) (27). The results associated with this examination are in whole or part based upon data generated by the TCGA Research Network. Factors that contributed to invasion and apoptosis were gathered through peer-reviewed sources and online databases such as GeneCard ® (28).

5. siRNA treatment for MDA-MB-231 and MCF7 cell lines

Twenty-four hours prior to transfection, $5x10^5$ cells (MDA-MB-231 and MCF7) were seeded in a six well plate. The protocol provided by Invitrogen™ for Lipofectamine® RNAiMAX was adapted for Silencer® Select TK1 s14160, Silencer™ Select negative control (scramble), and Silencer™ Select GAPDH positive control siRNA treatments. Treatment

wells were transfected with Lipofectamine® RNAiMAX, diluted in Opti-MEM™ which contained 25-30 pmol/ ~10 µm of TK1, scramble or GAPDH siRNA. The cells were incubated at 5% CO2 and 37°C for 6-8 hours in siRNA treatment and then washed once with PBS and allowed to recover in complete RPMI 1640 (supplemented with 10% FBS and 2mM glutamine) for ~16 hours. A second transfection with the same conditions was performed 24 hours following the first transfection and incubated for 6-8 hours before being washed once with PBS and placed in complete RPMI 1640 culture media. Transfected cells were harvested 24 hours after the second transfection for subsequent invasion and Western Blot analysis.

6. Cellular invasion assay

Cells were grown to exponential phase prior to the 24-hour analysis. Matrigel® from Corning® was also prepared in advanced and set prior to experimentation. Culture media supplemented with 5% FBS was placed in the top chambers, while the bottom chambers were seeded with 10% FBS media. Each chamber was inoculated with 5×10^4 cells in the upper chamber above the Matrigel® in a 16-well electronic polycarbonate membrane, 8 µm pore size cell invasion and migration plate (CIM-Plate® 16, Xcelligence ACEA Biosciences, Inc). Cells were incubated at 37°C and allowed to migrate for 24 h. Invasive cells were detected by cellular impedance of gold electrodes fused into 16-well plate as cells migrated from the upper to lower chamber. Kinetic measurements of invasive cells were calculated based on cell index (Cell Index (CI), where:

[Due to technical limitations, the formula could not be displayed here. Please see the supplementary files section to access the formula.]

Real-time cell analysis (RTCA, Xcelligence, ACEA Biosciences, Inc.) converted kinetic data to cell index for further analysis between cell lines in PRISM® (GraphPad Software, Inc.).

7. Cell lysate preparation and Western Blot

Cell lysate for siRNA treatments as well as wild type cell lines and TK1 knockdown cell line ($L133^{TK1-/-}$) were tested for presence of cytosolic TK1 via western blotting. Cells were grown to 100% confluency in a 150T sized flask and trypsinized prior to treatment with ~1.5 ml of NP40 lysis buffer from Invitrogen™ supplemented with protease inhibitor cocktail for 30 minutes on ice vortexing every 10 minutes. Cell lysate samples were aliquoted and stored at -80°C. The Pierce™ BCA Protein Assay Kit from Thermo Scientific™ was used according to manufacturer's instructions to quantify protein concentration of cell lysate samples. Protein concentration was analyzed on a BioTek® plate reader at 562nm. Western blot analysis was performed using ~30ug of cell lysate from respective samples. Samples were thawed on ice and prepared with SDS loading dye and water before being boiled for 5 minutes, ~30ug of protein were loaded per well. The samples were loaded into a 12% acrylamide SDS gel and placed at 90 V for 2–3 hours. Proteins were transferred onto a nitrocellulose membrane at 90 V for 50 minutes. The nitrocellulose membrane was blocked with 5% nonfat milk in PBS for 1 hour at room temperature (RT) on a rotating platform. All further washes and incubations were carried out on a rocking platform. Samples were washed in PBS three times for five minutes at RT and were incubated in either anti-TK1 commercial antibody (Abcam® 76495) or anti-GAPDH antibody (Cell Signaling® 14C10). All primary antibodies were incubated in a 1:1,000 dilution in PBS overnight at 4°. The membrane was washed three times in PBS for five minutes at room temperature and incubated with an HRP-goat anti-rabbit secondary antibody for 1 hour at 4°C

prior to imaging. The membrane was washed three times with PBS and exposed following manufacturer's instructions for Advansta WesternBright™ ECL horseradish peroxidase substrate. Western Blots were then exposed to film and developed. Protein size was determined by comparing to ExcelBand™ All Blue Broad Range Protein Marker from SMOBIO®.

8. CRISPR-Cas9 development for HCC 1806 TK1$^{-/-}$ cell line

CRISPR plasmid pSpCas9(BB)-2A-Puro (PX459) V2.04 was acquired from Addgene and streaked onto lysogeny broth (LB) ampicillin plates prior to isolation—this plasmid will be referred to as PX459. The plasmid was handled according to standard procedures. Guide RNAs (sgRNAs) were designed using suggestions provided by Addgene as well as online scoring sources such as CRISPOR tefor, CRISPR MIT, and CRISPR RGEN Tools (29-33) (Additional File 1).

9. CRISPR-Cas9 PX459 transfection

HCC 1806 cells were seeded with 5x10^5 in each well of a six-well plate and incubated overnight prior to transfecting PX459. Lipofectamine® LTX DNA Transfection Reagent (Thermo Scientific™, address, country) was used according to manufacturer's instructions for cell transfection. LTX reagent was diluted into Opti-MEM^{TM} to a 6% concentration. In a separate tube, DNA (9 ng) was diluted in PLUSTM reagent in a 1:1 ratio and added to 450 ul of Opti-MEM^{TM}. Both tubes were incubated for 5 minutes prior to adding the solution containing DNA to the LTX reagent in Opti-MEM^{TM} and were incubated together for 20 minutes. Treatment was added dropwise to corresponding wells for a final concentration of 3 ng PX459. Cells were incubated for 3 days at 37° C and 5% CO_2. Transfected cells were selected with puromycin (2ug/ml) until control cells were eliminated. Surviving transfected cells were then recovered in respective media according to proper culture techniques. Stable knockouts of TK1 were confirmed through Western Blotting (Figure 10).

10. Nitrophenyl phosphate cell proliferation assay

Standard growth curves were generated for each cell line (HCC 1806 and L133$^{TK1-/-}$). Cells were grown in 96-well plates at seeding densities from 0 to 1.2x10^3 cells per well, increasing by increments of 1x10^{3}cells. The culture medium was removed, and cells were washed once with 200 ul of PBS. To each well, 100 ul of buffer containing 0.1 M sodium acetate (pH 5.0), 0.1% Triton 100X, and 5mM p-nitrophenyl phosphate was added. The plates were placed in a 37°C incubator for 2 hours. The reaction was stopped with the addition of 20 ul of 1 M NaOH, and color development was assessed at 405 nm on a Biotek ® Synergy^{TM} HT microplate reader.

11. Glucose deprived and hypoxic apoptosis

HCC 1806 and L133$^{TK1-/-}$ cell lines were plated in 6 well plates with 5x10^5 cells per well. Cells were allowed to adhere to the plates (~2-3 hours) before being placed under glucose deprivation and hypoxic stress for 24 hours. Hypoxic stress

was induced with Cobalt (II) Chloride hexahydrate at a final concentration of 50 µM. The last 12 hours of the 24-hour incubation, 20 µM of camptothecin was introduced into positive control wells to induce apoptosis (Additional File 2). Apoptotic cells were identified through phosphatidylserine translocation to the outer membrane and measured by BD Pharmigen^{TM}, FITC Annexin V Apoptosis Detection Kit I. The tested samples were examined for Annexin V binding on a Beckman Coulter Cytoflex ® and results were analyzed using FlowJo ® software.

12. Apoptosis induced by DNA damage through hydrogen peroxide

HCC 1806 and L133$^{TK1-/-}$ cell lines were plated in 6 well plates with 5x10^5 cells per well. Cells were allowed to adhere to the plates (~2-3 hours) before being placed under oxidative stress. Oxidative stress was introduced with hydrogen peroxide treatment for 4 hours at concentrations of 0 mM, 0.2 mM, 0.4 mM, 0.8 mM, and 1.6mM. Apoptotic cells were identified through phosphatidylserine translocation to the outer membrane and measured by BD Pharmigen^{TM}, FITC Annexin V Apoptosis Detection Kit I. The tested samples were examined for Annexin V binding on a Beckman Coulter Cytoflex ® and results were analyzed using FlowJo ® software.

13. Flow cytometry

Flow cytometry was used to test positive controls for apoptosis experiments used in compensation. Harvested cells used in apoptotic experiments (HCC 1806 and L133$^{TK1-/-}$) were harvested after accutase treatment. The cells were then washed twice with PBS and resuspended in 100 µl of 1x binding buffer (BD Pharmigen^{TM} item 556547). Using indirect staining techniques followed from Abcam®, 5x10^5 cells were stained indirectly with a mouse IgG antibody against human HLA-A,B,C Antibody 311402 Biolegend® for 30 minutes on ice. The cells were washed twice with 1 ml of PBS. Cells were stained with secondary IgG goat anti-mouse Abcam® 6785 FITC conjugated antibody for 30 minutes on ice in the dark. Before examination on the flow cytometer, samples were washed 3 times with PBS to remove unbound secondary antibody.

Samples for propidium iodide (PI) positive control were also included in apoptotic experiments. The samples for PI control were washed twice with PBS and resuspended in 100 µl of 1x binding buffer. To every tube, 100 µl of 0.1% triton was added to each tube and mixed well prior to a 15-minute incubation on ice. Following the 15-minute incubation, 200 µl of PI were added to each tube and incubated at room temperature for 30 minutes.

For all samples, we collected ≥ 10,000 events per sample (Cytoflex ® Beckman Coulter, Indianapolis, Indiana, USA), and the data were analyzed using the FlowJo ® software (FlowJo, Inc., Ashland, OR, USA).

14. Cell cycle analysis

To detect differences in cell cycle between wild type and TK1 knockdown cell types, HCC 1806 and L133$^{TK1-/-}$ cells were plated with a total of 3.5x10^5 cells in each well of a six well plate 24 hours prior to cell cycle analysis. Samples were trypsinized and washed twice with PBS prior to fixation in 4% paraformaldehyde for 15 minutes at 4°C. Following

fixation, samples were washed once with PBS and placed in 70% methanol overnight. All samples were washed a final time in PBS and treated with RNAse. Test samples were treated with propidium idodide for 30 minutes at 4°C. Positive staining for propidium idodide was detected on a Beckman Coulter Cytoflex ® and cell cycle analysis was performed in FlowJo, LLC Cell Cycle Platform software®.

15. Heatmap generation testing correlations of TK1 to cancer promoting genes

Upper quartile-normalized RNA-sequencing read counts were retrieved from The Cancer Genome Atlas (34, 35) using the TCGAbiolinks software package (36) . Counts for 459 protein-coding genes that were manually-curated for participation in invasion, apoptosis, or progression were saved for nine cancer types including: breast, colon, lung, urinary bladder, pancreatic, uterine, thyroid, kidney, and prostate. Separate correlation matrices and standard deviations were calculated for these genes in each cancer type (Additional File 3). TK1 correlation values that were greater than or equal to +/- two standard deviations from the mean for each cancer type were used as input for heatmap visualization.

Results

1. TK1 expression between normal and cancer samples

Across all cancer types, metastatic cell lines had higher levels of TK1 when compared to primary (p=0.0001) cell lines (Figure 1). Looking at TK1 expression in RNA-seq TCGA data, TK1 showed higher elevation in 20 out of 24 cancer tissues (Figure 2). While a majority of cancers had elevated levels of TK1, there were four cancer types with insignificant or lower expression: kidney chromophobe, cholangiocarcinoma, thymoma, skin cutaneous melanoma. Despite this difference, we observed that there was wide variation between the different cancer cell lines and cancer types and decided to focus further studies solely in breast cancer due to its aggressive nature and high levels of TK1 (Figure 3). A breast tissue array (n=96) which included infiltrating lobular, invasive ductal as well as matched metastatic and adjacent normal was tested for levels of TK1 against positive and negative controls. Similar to the results of our bioinformatic studies, we showed that metastatic ductal and lobular patient samples were higher overall for TK1 expression when compared to normal and primary breast tissue samples (p <0.0001) (Figure 4). Indicating that TK1 was higher with more aggressive tissue types.

Figure 1: Comparing TK1 levels in metastatic and primary cancer cell lines
RNA-seq data from Cancer Cell Line Encyclopedia (CCLE) for primary and metastatic cell lines were analyzed for TK1. Data was mined from a genomic RNA-seq database for well characterized cell lines. Prior to being analyzed, cell lines were categorized into primary and metastatic subgroups. Metastatic cell lines showed a significantly higher level for cytosolic TK1 than primary cell lines.

Figure 2*:* Expression of TK1 across TCGA cancers

Examining TK1 expression through RNA-seq data pulled from The Cancer Genome in various cancer types compared to normal samples. In several cancer types TK1 expression was significantly higher when compared to normal samples.

Figure 3: TK1 levels in normal breast tissue and primary BRCA tumor

Comparing transcript levels of TK1 in normal and BRCA patients. A significant difference is present between normal and primary tumor samples when evaluating TK1.

Figure 4: Immunohistochemistry staining of TK1 in invasive ductal and infiltrating lobular with matched metastatic and adjacent normal samples.

Tissue samples from invasive ductal and infiltrating lobular carcinoma patients with matching normal and metastatic samples were stained for TK1.

1. ANOVA test computed in PRISM testing differences between means. Metastatic had a higher presence of TK1 in comparison to normal tissue samples (p value <0.0001).
2. a) GADPH control b) normal human isotype c) invasive ductal d) metastatic ductal e) infiltrating lobular f) metastatic lobular

2. Effects of TK1 on cellular invasion

As TK1 has shown significant contributions to protein networks involved in cellular invasion, we tested for correlations between TK1 and factors known to aid in invasion. Of the 47 proteins examined, we found that 18 were positively correlated and 25 were negatively correlated to TK1 ($p \leq 0.05$) (Figure 5 and Table 1).

Table 1: Correlations between TK1 and invasive factors in BRCA RNA-seq patient data

Negative Correlations								
Protein	Correlation	P value	Protein	Correlation	P value	Protein	Correlation	P value
ETS2	-0.176	4.43E-09	MMP10	-0.099	9.75E-04	VIM	-0.074	1.44E-02
JUN	-0.105	4.84E-04	MMP16	-0.368	0.00E+00	CTNNB1	-0.275	2.28E-20
TIMP2	-0.208	3.60E-12	MMP17	-0.075	1.24E-02	MMP23	-0.201	1.76E-11
TIMP3	-0.257	5.46E-18	MMP19	-0.141	2.70E-06	MMP2	-0.234	4.80E-15
TIMP4	-0.263	8.04E-19	ETS1	-0.208	4.07E-12	MMP3	-0.099	1.06E-03
SNAI2	-0.246	1.80E-16	PRKB	-0.098	1.21E-03	LAMC1	-0.246	1.60E-16
GSC	-0.108	3.41E-04	PIK3CA	-0.202	1.54E-11	Zeb2	-0.336	0
FoxC2	-0.153	3.42E-07	Twist1	-0.105	4.93E-04	NFKB1	-0.330	0
			Twist2	-0.139	3.65E-06			
Positive Correlations								
Protein	Correlation	P value	Protein	Correlation	P value	Protein	Correlation	P value
ApoE	0.204	8.69E-12	TCF3	0.220	2.07E-13	MMP8	0.114	1.51E-04
ITGB2	0.092	2.32E-03	CDH1	0.090	2.77E-03	MMP9	0.220	2.11E-13
ITGB7	0.202	1.47E-11	CTSD	0.106	4.50E-04	MMP12	0.226	3.14E-14
CD24	0.062	4.06E-02	CTSB	0.115	1.38E-04	MMP15	0.197	4.78E-11
F11R	0.220	2.06E-13	PLAU	0.066	2.90E-02	BSG	0.319	0.00E+00
Snai1	0.195	6.88E-11	MMP1	0.303	8.99E-25	TNF	0.149	6.61E-07

RNA-seq data from The Cancer Genome Atlas (TCGA) evaluated in BRCA patients (n=1095) for correlations between invasive proteins and TK1. The RNA-seq data was analyzed using the TIMER program developed by Li et al. Correlation strength and p value for negative and positive correlations between TK1 and invasion factors are shown for significant correlations ($p \leq .05$).

Figure 5: Visual depiction of correlation strength between TK1 and invasive factors

RNA-seq data from The Cancer Genome Atlas (TCGA) evaluated in BRCA patients (n=1095) evaluating correlations between invasive proteins and TK1. Significant Spearman correlations are shown for positive (n= 18) and negative (n=25) coefficients ($p \leq .05$). Stronger correlations are denoted by a horizontal asymptote at one standard deviation 0.2 and -0.2.

Despite no observable strong pattern between TK1 and positive or negative correlations, we decided to evaluate TK1 affects *in vitro* on cellular invasion based on findings from others previous research (18-20) . Using Xcelligence technology, we measured the effect of TK1 on cellular invasion over a 24-hour period. We compared wild-type cell lines to corresponding treatment of siRNA targeting TK1 and siRNA controls: scramble (negative control) and GAPDH (positive control) (Figure 6). When compared to the wild-type MDA-MB-231 cell line, MDA-MB-231 TK1 knockdown cells showed increased cellular invasion ($p < 0.0001$) (Figure 7).

Figure 6: Confirming TK1-/- in siRNA treated cell lines MDA-MB-231 and MCF7
Western blot analysis of siRNA treated HCC 1806 and MDA-MB-231 cells.

1. Blotting for GAPDH

2. Blotting for TK1.

Figure 7: Cellular invasion assay comparing MDA-MB-231 wild type and TK1-/- cells

Invasion of 24-hour analysis comparing siRNA treatments in MDA-MB-231 and MCF7 human breast cell lines.

1. ANOVA test computed in PRISM testing differences between means (p value ≤ 0.01).
2. Cellular invasion of breast cell lines was monitored over 24 hours through a 4% Matrigel.

To determine whether the transfection itself was influencing the ability of the cells to invade, we tested the cellular invasion of breast cancer cell line HCC 1806 and the CRISPR-Cas9 HCC 1806 treated cell line ($L133^{TK1-/-}$). To ensure the TK1 knockout did not affect cellular proliferation, we performed a nitrophenyl phosphate cell proliferation assay and confirmed there was no difference in frequency (doubling time in 24 hours) between HCC-1806 and $L133^{TK1-/-}$ (Figure 8). Further testing in which we compared the cellular invasion of $L133^{TK1-/-}$ and wild-type cell line HCC 1806 showed the same phenomena. We observed $L133^{TK1-/-}$ cells had increased invasion when compared to HCC 1806 cells (Figure 9). We concluded that the siRNA treatment was not inhibiting cellular invasion and that the reduced levels of TK1 contributed to higher invasion potential.

Figure 8*:* CRISPR-Cas9 HCC 1806 $TK1^{-/-}$ western blot and nitrophenyl phosphate cell proliferation assay testing doubling time in 24 hours (frequency) for HCC 1806 and $L133^{TK1-/-}$ cells

Cellular proliferation effect of CRISPR-cas9 TK1 knockdown treatment.

1. Nitrophenyl phosphate cell proliferation assay was used to identify differences in cellular proliferation. Standard curves were developed for HCC 1806 and $L133^{TK1-/-}$. Known seeding densities were plated and assayed for nitrophenol conversion at 405nm at 24 hours. The average frequency, or number of cell cycle phases per day, was calculated for HCC 1806 and $L133^{TK1-/-}$. No significant difference was found between the two cell lines.
2. Western blot identifying TK1 expression in $L133^{TK1-/-}$ and HCC 1806, no significant amount of TK1 was identified in $L133^{TK1-/-}$ samples.

Figure 9: Cellular invasion analysis comparing HCC 1806 and $L133^{TK1-/-}$ cell lines

Invasion 24-hour analysis comparing HCC 1806 and CRISPR-Cas9 $L133^{TK1-/-}$ cell line.

1. ANOVA test computed in PRISM testing differences between means (p value ≤ 0.0001).
2. Cellular invasion of breast cell lines was monitored over 24 hours through a 4% Matrigel.

3. Examining tumor survival of TK1 effects on apoptosis

Although the contribution of TK1 directly to cellular invasion was inhibitory, we considered that it might indirectly influence invasion by promoting cell survival. During our examination of correlations between TK1 and invasive factors, our peripheral bioinformatic research showed strong correlations between TK1 to apoptotic factors such as survivin or BIRC5. We proposed high levels of TK1 were a result of reduced inhibitory interactions of Rb and p21 which would promote growth and provide survival signals within the cell (Figure 10).

Figure 10: Correlation plots of TK1 vs. RB1, CDKN1A, and E2F1 in BRCA patients

RNA-seq data evaluated in BRCA patients (n=1095) for correlations between TK1 and regulatory factors: RB (RB1), p21 (CDKNA1), and E2F (E2F1) (p value ≤ 0.05). As TK1 expression increases, inhibitory factors RB and p21 decrease and transcription factor E2F increases.

Bioinformatic research was conducted to test for correlations between TK1 and apoptotic factors (n=160) identified using the PathCards database (28) . We identified an overall negative correlation between TK1 and pro-apoptotic factors (Figure 11 and Table 2). Using the online program Panther Classification System developed by Huaiyu Mi et al., we found that 47 proteins were involved in glucose deprived or oxidative stress response (37).

Table 2: Correlations between TK1 and apoptotic factors in BRCA RNA-seq patient data

RNA-seq data evaluated in BRCA patients (n=1095) for correlations between apoptotic factors and TK1. Rna-seq expression was analyzed using TIMER program developed by Li et al. (p value ≤ 0.05).

Figure 11: Visual depiction of correlation strength and between TK1 and apoptotic factors

RNA-seq data evaluated in BRCA patients (n=1095) for correlations between apoptotic factors and TK1. Significant Spearman correlations (p value ≤ 0.05) are shown for positive (n= 37) and negative (n=90) coefficients. Stronger correlations are denoted by a horizontal asymptote at one standard deviation 0.2 and -0.2.

We then measured cellular survival through apoptosis under metabolic and DNA stress in HCC 1806 and L133$^{TK1-/-}$ cell lines. Following glucose deprivation and hypoxic treatment for 24 hours, we saw an increase in apoptosis in the wild type HCC 1806 cell line when compared to L133$^{TK1-/-}$ ($p<0.0001$) (Figure 12). We then assessed a known role of TK1 in DNA repair and evaluated the survival of HCC 1806 cells compared to L133$^{TK1-/-}$ cells when exposed to varying concentrations of hydrogen peroxide. Between all concentrations of hydrogen peroxide treatments (0, 0.2, 0.4, 0.8, and 1.6 μM), HCC 1806 cells showed no differences in apoptosis (Figure 13). In L133$^{TK1-/-}$ cells we saw increasing levels of apoptosis with increased concentrations of hydrogen peroxide ($p < 0.05$) (Figure 13).

Figure 12: Annexin V results testing glucose deprived and hypoxic induced apoptosis in HCC 1806 and L133$^{TK1-/-}$ cell lines

Flow cytometry results of apoptosis with glucose deprivation and hypoxia treatment. Apoptosis is measured by Annexin VFITC staining.

1. Comparing means of HCC 1806 controls and samples
2. Comparing means of L133$^{TK1-/-}$ controls and samples
3. CRISPRgRNA-TK1 treated cell line L133$^{TK1-/-}$ has increased apoptosis when compared to HCC 1806 cell line.

Figure 13: Annexin V results from oxidative induced apoptosis using hydrogen peroxide in HCC 1806 and L133$^{TK1-/-}$ cell lines

Flow cytometry results of apoptosis with hydrogen peroxide treatment. Apoptosis is measured by Annexin VFITC staining.

1. Comparing means of HCC 1806 controls and samples.
2. Comparing means of L133$^{TK1-/-}$ controls and samples.
3. L133$^{TK1-/-}$ cells have increased apoptosis when compared to HCC 1806 cell line with high DNA damage.

Several DNA damage pathways were identified to positively correlate to TK1 levels in BRCA RNA-seq patient data including BRCA1 and BRCA2 as well as 14-3-3 factors and ATM DNA damage checkpoint G1/S (Figure 14). The results from the apoptotic assay under DNA stress and bioinformatic analysis showed that TK1 was promoting survival in cancer cells during cellular DNA damage—these results are well supported by other research studies (5, 38, 39).

Figure 14*:* Visual depiction of correlation strength between TK1 and different DNA damage pathways

RNA-seq data from The Cancer Genome Atlas (TCGA) evaluated in BRCA patients (n=1095) evaluating correlations between apoptotic pathways regulated by DNA damage factors and TK1. Stronger correlations are denoted by a horizontal asymptote at one standard deviation 0.2 and -0.2.

1. ATM checkpoint factors
2. BRCA1 and BRCA2 factors
3. 14-3-3 factors

4. Regulation of TK1 and its suggestions in TK1$^{-/-}$ cell cycle phases

To understand the reason for our observations, we decided to explore TK1 regulation. We first observed that normal tissue samples had higher levels of methylation compared to BRCA primary tumor samples ($p= 1.1 \times 10^{-16}$) (Figure 15). From the PathCard database we obtained factors within the cell cycle checkpoint pathway (n=181) and evaluated BRCA RNA-seq patient data (n=1093) for correlations between TK1 and cell cycle checkpoint regulation factors (n=150). These results exhibited strong positive correlations to TK1 levels ($p \leq .05$) (Figure 16 and Table 3). We

concluded that TK1 upregulation could be a result of decreased methylation at the promoter region and mis-regulation by cell cycle checkpoint factors.

Figure 15: Comparing methylation at the TK1 promoter between normal tissue and primary tumor samples

Promoter methylation level of TK1 in BRCA patients. The beta value indicates level of dna methylation ranging from 0 (unmethylated) to 1 (fully methylated).

Figure 16: Visual depiction of correlation strength between TK1 and Cell Cycle Checkpoint Factors

RNA-seq data evaluated in BRCA patients (n=1095) for correlations between cell cycle checkpoint factors and TK1. Significant Spearman correlations (p value ≤ 0.05) are shown for positive (n= 150) and negative (n=30) coefficients. Stronger correlations are denoted by a horizontal asymptote at one standard deviation 0.2 and -0.2.

Table 3: Correlations between TK1 and cell cycle checkpoint factors in BRCA RNA-seq patient data

RNA-seq data evaluated in BRCA patients (n=1095) for correlations between cell cycle checkpoint factors and TK1. RNA-seq expression was analyzed using TIMER program developed by Li et al. (p value ≤ 0.05).

To observe possible changes in cell cycle phases between L133$^{TK1-/-}$ and HCC 1806 cells we performed cell cycle analysis. From our analysis, we saw a higher population of L133$^{TK1-/-}$ cells in S phase compared to HCC 1806 cells (Figure 17). Cell cycle analysis provided additional information supporting our hypothesis that increased levels of TK1 were linked to regulation by cell cycle checkpoint proteins. From these results we also concluded that survival signals during S phase explained the decrease in apoptosis and increase in cellular invasion for L133$^{TK1-/-}$ cells.

Figure 2-17: Cell cycle results analyzing cell populations in G1, S and G2 between HCC 1806 and L133$^{TK1-/-}$ cells

Figure 2-17: Flow cytometry results of cell cycle analysis measuring propidium iodide staining.

1. Comparing means of HCC 1806 controls and samples.
2. Comparing means of L133$^{TK1-/-}$ controls and samples.
3. CRISPR-Cas9 treated cell line L133$^{TK1-/-}$ has increased apoptosis when compared to HCC 1806 cell line.

5. Exploring factors in invasion, apoptosis and progression

As a result of our findings in cellular invasion and apoptotic assays, we supposed that TK1 was reliant on other factors to aid in cancer pathogenesis. RNA-sequencing read counts were assessed for 459 protein-coding genes in nine different TCGA cancers. Among the factors assessed, there were n=126 statistically significant correlations to TK1 (Figure 18). Among the strongest correlations are proteins such as BIRC5, BRCA1, H2AFX, CHEK2 and cyclins A2, B1 and B2. Correlations included in the heatmap (figure) were greater than or equal to +/- two standard deviations from the mean for each cancer type.

Figure 18: Heatmap of TK1 correlations to invasive, apoptotic and cancer promoting genes across nine different TCGA cancers

Heatmap is depicting correlation strength to TK1 and cancer progressive genes. Genes shown are +/- two standard deviations away from the mean. Correlations were assessed from RNA-sequencing read counts in nine different TCGA cancers. Abbreviations of cancer type are provided below.

Discussion

Breast cancer is among some of the most aggressive cancer types with 20–30% of diagnosed tumors becoming metastatic; in fact, metastasis is the main cause of death among all cancer patients (40). To improve patient treatment, biomarkers are continually studied to improve clinical procedures for diagnosis and prognosis. In breast cancer specifically, biomarkers used to identify patient tumors include 15–3 (CA 15–3), cancer antigen 125 (CA 125), and carcinoembryonic antigen (CEA)(16). TK1 is a relatively newer cellular proliferation marker that shows potential to identify malignant cells for various cancer types including breast (6–8, 13, 15, 17, 41, 42).

Beyond the known function of TK1 in cellular proliferation and its potential as a cancer biomarker, the contribution of TK1 to tumor progression is largely unknown. A few research teams have designated that TK1 is a key player in a network affecting cellular invasion in breast cancer and tumor progression in both prostate and adrenocortical carcinoma (18–20). The results from these studies show TK1 in tandem with a network or group of proteins affect downstream processes. We determined to evaluate and quantify the individual role of TK1, both bioinformatically and *in vitro,* in cancer progression—specifically measuring cellular invasion and cell survival.

From our analysis in TCGA RNA-seq patient data across multiple cancer types, there were high levels of TK1 when compared to normal tissue. We saw a similar trend when comparing invasive ductal and infiltrating lobular to matched metastatic tissue samples in breast cancer patients. This could indicate that evolving cells preferentially select for upregulation of TK1 possibly as an advantage for tumor progression.

Because we saw higher levels of TK1 in matched metastatic breast tissue samples, we questioned if TK1 played an integral role in cell invasion. Tilli et al., previously determined that a network of five different proteins, counting TK1, were influential in MDA-MB–231 cellular invasion (18). From our cellular invasion assays comparing TK1 knockdown or knockout cell lines to wild-type cells lines, we demonstrated that when analyzed individually, TK1 played an inhibitory role during cellular invasion. However, we recognized that the invasive environment tested in this study was reliant on an FBS gradient and TK1 may have altering affects dependent on the conditions. There are several environmental factors affecting cancer survival including glucose deprivation, hypoxia and immune cell infiltration. In the future, we plan to assess different invasive conditions in the same manner tested with the FBS gradient and using appropriate 3D culture systems.

These results differed from reported studies evaluating TK1 effect on cellular invasion within a protein network. When closely examining differentially expressed genes identified by previous research studies, there appeared to be commonalities in protein functions affecting invasion. The study by Ashalbi, et. al summarized that there were two highly enriched pathways which consisted of cell cycle proteins and pyrimidine nucleoside salvage enzymes (20). Song et al. reported similar enriched pathways (19). We suggest that proteins from these enriched pathways work in tandem with TK1 to promote cellular invasion and when examined individually, TK1 does not elicit the same response.

Briefly, we evaluated the correlation strength for RNA-sequencing reads of proteins tested above for correlations to TK1 in multiple cancer types. To effectively identify correlation strength between TK1 and these factors, only factors that were two standard deviations above and below the mean were included as input for the visual heatmap (Figure 18). Among the strongest correlations across multiple cancer types were BIRC5, H2AFX, LMNB1 and 2, cyclins A2, B1 and B2, BRCA1, and CHEK2. We suggest that these are potential proteins that interact with TK1 and could be studied as a protein network.

We questioned if TK1 was inhibiting cellular invasion, perhaps its individual contribution to tumor progression was linked to promoting cell survival. When exposed to a glucose deprived and hypoxic environment, we saw a decrease in apoptosis in the CRISPR-Cas9 knockout cell line. We were surprised by this in light of our bioinformatic study and wanted to see if saw major differences in TK1 deficient cells based on known roles of the enzyme, such as in DNA repair. When measuring apoptosis from oxidative damage in L133$^{TK1-/-}$ cells and HCC 1806, we observed that the wild type HCC 1806 cells had less apoptosis in high concentrations of hydrogen peroxide. These results are supported by other sources which indicate that TK1 contributes cancer cell survival during DNA damage(9, 10, 38, 39).

We then further explored possibly reasons why we saw a decrease in cellular invasion in L133$^{TK1-/-}$ cells and a decrease in apoptosis from glucose and hypoxic (metabolic) stress in L133$^{TK1-/-}$ cells. First, we examined cell cycle phases through propidium iodide staining in wild type HCC 1806 and CRISP-Cas9 L133$^{TK1-/-}$. Interestingly, we identified L133$^{TK1-/-}$ cells had a higher population in S phase when evaluated in normal growth conditions compared to HCC 1806 cells. We attribute the higher levels of cellular invasion in the L133$^{TK1-/-}$ cell line and decrease in hypoxic and glucose deprived induced apoptosis to this shift in cell population to S phase. The shift towards S phase, would promote survival and therefore prevent apoptosis (43–46).

Several research groups have indicated that cell growth encourages cell survival and decreases the opportunity for cell death or apoptosis (47–52). Based on differences in G1 and S between HCC 1806 and L133$^{TK1-/-}$, we propose that TK1 may be influencing cell cycle transitions, specifically S to G2. The shift may be a result of decreased availability of dTTP provided by TK1, locking the cells in S phase or a result of high TK1 levels present within the cell.

We also explored the possible mechanism behind increased levels of TK1. From extracted online results, we showed that there was a decrease in methylation in tumor tissue samples at the promoter region when compared to normal tissue. We also observed a strong positive correlation to cell cycle checkpoint pathway proteins and TK1 in BRCA RNA-seq patient data. We suggest that TK1 in cancer cells is still connected to cell cycle factors, but that the upregulation of TK1 is the result of transcription and protein misregulation. From an additional bioinformatic study, we presume that one of the specific cell cycle checkpoint pathway proteins interacting with TK1 is CHEK2, responsible for cell cycle control and mediating DNA damage repair (53).

Another way in which cell proliferation is mediated is through the MAPK/ERK signaling pathway (49). Based on strong negative correlations in BRCA RNA seq patient data between MAPK/ERK signaling factors and TK1, we high levels of TK1 could also be a result of mutations in the MAPK/ERK signaling pathway (Additional File 4). These mutations could lead to overexpression of E2F and reduced interactions of TK1 with pRB and p21(41).

After reflecting on our study, we suggest that isolating TK1 effects to understand its effect on cancer pathogenesis is deficient. Instead, we propose that TK1 may have alternate roles from DNA repair and pyrimidine salvage, but they are reliant on interactions with other proteins. Using a bioinformatic approach initially, we plan to examine RNA-sequencing to identify enriched pathways that are affected directly or indirectly by TK1. Once specific pathways are identified, *in vitro* experiments which block these pathways could confirm TK1 interactions within the cancer cell promoting its development. Through identifying enriched pathways, we aim to also elucidate the mechanism for increased levels of TK1 and the reasons for S phase arrest in TK1 deficient cells.

The upregulation of TK1 is shown to be an early event and elevated across several cancer types. The elevation of anabolic enzymes such as TK1 is potentially selected for in multiple cancer types as an advantage in tumorigenesis (6). TK1 is mentioned as part of a protein network and/or enriched DEG group that is linked to cellular invasion and tumor progression (18–20). These networks and DEG groups mentioned in cellular invasion and tumor progression studies consistently show factors involved in cell cycle regulation, nucleotide salvage, structural integrity, and cell adhesion. Continuing to elucidate the evolutionary advantage of increased availability of TK1 in cancer cells could point to improved drug treatments and therapies for various cancer types.

Conclusion

Thymidine kinase 1 (TK1) has been shown to be present in the serum of patients of several different cancer types and has high potential as a cancer biomarker for diagnosis and prognosis. Recent studies have postulated that TK1 may contribute to cancer pathogenesis in breast, lung and colon. We aimed to identify the effects of TK1 *in vitro* in breast cancer cells on cellular invasion and survival by comparing wild type cell lines to $TK1^{-/-}$ cells. Our results show that TK1 does provide protective affects during DNA damage, but that high levels of TK1 may promote apoptosis in certain conditions. We also see that high levels of TK1 prevent invasion in both $siRNA^{TK1-/-}$ and $CRISPR\text{-}Cas9^{TK1-/-}$ cells. We attribute the inhibited invasion and increased apoptosis to the shift in S phase in $TK1^{-/-}$ cell types. From bioinformatic analysis, we propose that cancer progression effects of TK1 are reliant on other factors. Evaluating TK1 effects within a protein network will be necessary to elucidate the direct or indirect pathways it influences to help aid in cancer pathogenesis and progression.

Additional Files

Additional File 1

- File format: PDF, figure
- Title: Visual depiction of CRISPR-Cas9 PX459 plasmid and designed guide RNAs
- Description of data:

CRISPR-Cas9 plasmid PX459 from Addgene

1. Visual depiction of PX459 and plasmid elements for transcription, translation and selection
2. Four guide RNAs were designed and tested, guide RNA 1 was the insert selected for future use.

Additional File 2

- File format: PDF, figure
- Title: Flow cytometry positive controls used in apoptosis analysis
- Description of data:

Positive controls are shown for apoptotic experiments, camptothecin was only used as an apoptotic control in metabolic stress experiments.

Additional File 3

- File format: .xls, table
- Title: Correlations of TK1 to invasive, apoptotic, and cancer progressive genes to TCGA cancer types
- Description: Correlation values for proteins factors (n=126) associated to Figure 18 are given in the table for two standard deviations above and below the calculated mean.

Additional File 4:

- File format: Word Table

Negative Correlations							
Protein	**Correlation**	**Protein**	**Correlation**	**Protein**	**Correlation**	**Protein**	**Correlation**
LAMA2	-0.513	COL14A1	-0.458	TGFB3	-0.432	FGF10	-0.414
APH1B	-0.501	PPP1R12B	-0.451	ECM2	-0.427	ATM	-0.414
PDGFD	-0.500	HGF	-0.448	ARHGEF12	-0.424	GNG12	-0.411
CX3CR1	-0.500	CACNA1D	-0.445	TEK	-0.423	TEAD1	-0.410
DOCK1	-0.472	IGF1	-0.444	TCF4	-0.423	BCL2	-0.409
BMPR2	-0.468	ELK3	-0.442	FOXO1	-0.421	SMAD5	-0.404
ZEB1	-0.468	OGN	-0.441	CACNA1C	-0.420	FGF14	-0.403
SEMA5A	-0.459	RPS6KA2	-0.434	ATF7	-0.420	IRS1	-0.402
RASA1	-0.458	TGFBR2	-0.433	TCF12	-0.418	LIFR	-0.401
Positive Correlations							
Protein	**Correlation**	**Protein**	**Correlation**	**Protein**	**Correlation**	**Protein**	**Correlation**
CDK2	0.409	HIST1H3B	0.456	CFL1	0.480	TCF19	0.616
PPP2R5D	0.409	RAC3	0.457	CDK4	0.485	CDK1	0.623
HDGF	0.439	CIT	0.462	DIAPH3	0.499	AURKA	0.628
TUBG1	0.455	CDC25B	0.462	CHEK2	0.535	CDC25C	0.635
PPP1R14B	0.473	CDKN2D	0.464	CHEK1	0.574	CDC25A	0.638
FANCD2	0.468	ARHGDIA	0.467	STMN1	0.574	RAD51	0.670
E2F2	0.616	CCNE2	0.468	CCNE1	0.578	E2F1	0.695
						AURKB	0.725

- Title: Correlations of TK1 to MAPK/ERK Pathway factors in BRCA RNA-seq patient data (n=1095)
- Description: Correlations values are provided for MAPK/ERK factors that are two standard deviations above and below the calculated mean.

Abbreviations

COAD = Colon cancer

LUAD = Lung cancer

UCEC = Uterine cancer

BLCA = Urinary bladder cancer

PAAD = Pancreatic cancer

BRCA = Breast cancer

KIRC = Kidney cancer

THCA = Thyroid cancer

PRAD = Prostate cancer

Declarations

1. Ethics approval and consent to participate

Not applicable

2. Consent for publication

Not applicable

3. Availability of data and materials

The datasets generated analyzed during the current study are available in the The Cancer Genome Atlas database and TIMER program developed by Li et al(26, 34, 35).

4. Competing interests

Not applicable

5. Funding

Funding was provided by funds from Brigham Young University and Thunder Biotech.

6. Authors' contributions

EB was the major contributor to research design, data collection, data analysis and writing the manuscript. MT aided in research design and editing the manuscript. KT performed all of the invasion assays and assisted in cellular invasion analysis. CA and RE both assisted in cell culture, western blots, and sample preparation for flow cytometry. BP provided the heatmap graphic and analysis of cancer promoting genes across cancer types. JA assisted in invasion analysis design and editing the manuscript. KO was a contributor in research design and editing the final manuscript. All authors have read and approve the final manuscript.

7. Acknowledgements

- Scott Weber
- Richard Robison

References

1.Bollum FJ, Potter VR. Nucleic acid metabolism in regenerating rat liver. VI. Soluble enzymes which convert thymidine to thymidine phosphates and DNA. Cancer research. 1959;19(5):561–5.

2.Weber G, Nagai M, Natsumeda Y, Ichikawa S, Nakamura H, Eble JN, et al. Regulation of de novo and salvage pathways in chemotherapy. Advances in enzyme regulation. 1991;31:45–67.

3.Engelking LR. Chapter 15 - Purine Biosynthesis. In: Engelking LR, editor. Textbook of Veterinary Physiological Chemistry (Third Edition). Boston: Academic Press; 2015. p. 88–92.

4.Puigserver P. Chapter 7 - Signaling Transduction and Metabolomics. In: Hoffman R, Benz EJ, Silberstein LE, Heslop HE, Weitz JI, Anastasi J, et al., editors. Hematology (Seventh Edition): Elsevier; 2018. p. 68–78.

5.Chen YL, Eriksson S, Chang ZF. Regulation and functional contribution of thymidine kinase 1 in repair of DNA damage. The Journal of biological chemistry. 2010;285(35):27327–35.

6.Munch-Petersen B, Cloos L, Jensen HK, Tyrsted G. Human thymidine kinase 1. Regulation in normal and malignant cells. Advances in enzyme regulation. 1995;35:69–89.

7.Topolcan O, Holubec L. The role of thymidine kinase in cancer diseases. Expert Opinion on Medical Diagnostics. 2008;2(2):129–41.

8.Zhou J, He E, Skog S. The proliferation marker thymidine kinase 1 in clinical use. Mol Clin Oncol. 2013;1(1):18–28.

9.Fischer M, Quaas M, Steiner L, Engeland K. The p53-p21-DREAM-CDE/CHR pathway regulates G2/M cell cycle genes. Nucleic Acids Res. 2016;44(1):164–74.

10.Engeland K. Cell cycle arrest through indirect transcriptional repression by p53: I have a DREAM. Cell death and differentiation. 2018;25(1):114–32.

11.Cai Z, Liu Q. Cell Cycle Regulation in Treatment of Breast Cancer. Advances in experimental medicine and biology. 2017;1026:251–70.

12.Collins K, Jacks T, Pavletich NP. The cell cycle and cancer. Proceedings of the National Academy of Sciences. 1997;94(7):2776.

13.Otto T, Sicinski P. Cell cycle proteins as promising targets in cancer therapy. Nature reviews Cancer. 2017;17(2):93–115.

14.Alegre MM, Robison RA, O'Neill KL. Thymidine kinase 1 upregulation is an early event in breast tumor formation. J Oncol. 2012;2012:575647-.

15.Ning S, Wei W, Li J, Hou B, Zhong J, Xie Y, et al. Clinical significance and diagnostic capacity of serum TK1, CEA, CA 19–9 and CA 72–4 levels in gastric and colorectal cancer patients. J Cancer. 2018;9(3):494–501.

16.Jiang ZF, Wang M, Xu JL. Thymidine kinase 1 combined with CEA, CYFRA21–1 and NSE improved its diagnostic value for lung cancer. Life sciences. 2018;194:1–6.

17.Xiang Y, Zeng H, Liu X, Zhou H, Luo L, Duan C, et al. Thymidine kinase 1 as a diagnostic tumor marker is of moderate value in cancer patients: A meta-analysis. Biomedical reports. 2013;1(4):629–37.

18.Tilli TM, Carels N, Tuszynski JA, Pasdar M. Validation of a network-based strategy for the optimization of combinatorial target selection in breast cancer therapy: siRNA knockdown of network targets in MDA-MB–231 cells as an in vitro model for inhibition of tumor development. Oncotarget. 2016;7(39)(1949–2553 (Electronic)):63189–203.

19.Song ZY, Chao F, Zhuo Z, Ma Z, Li W, Chen G. Identification of hub genes in prostate cancer using robust rank aggregation and weighted gene co-expression network analysis. AGING. 2019;11(13)(1945–4589 (Electronic)):4736–56.

20.Alshabi AM, Vastrad B, Shaikh IA, Vastrad C. Identification of important invasion and proliferation related genes in adrenocortical carcinoma. Med Oncol. 2019;36(9):73.

21.Chandrashekar DS, Bashel B, Balasubramanya SAH, Creighton CJ, Ponce-Rodriguez I, Chakravarthi B, et al. UALCAN: A Portal for Facilitating Tumor Subgroup Gene Expression and Survival Analyses. Neoplasia (New York, NY). 2017;19(8):649–58.

22.Zhu Y, Qiu P, Ji Y. TCGA-Assembler: open-source software for retrieving and processing TCGA data. Nature Methods. 2014;11(6):599–600.

23.Barretina J, Caponigro G, Stransky N, Venkatesan K, Margolin AA, Kim S, et al. The Cancer Cell Line Encyclopedia enables predictive modelling of anticancer drug sensitivity. Nature. 2012;483:603.

24.Townsend MH, Felsted AM, Piccolo SR, Robison RA, O'Neill KL. Metastatic colon adenocarcinoma has a significantly elevated expression of IL–10 compared with primary colon adenocarcinoma tumors. Cancer Biology & Therapy. 2018;19(10):913–20.

25.Schneider CA, Rasband WS, Eliceiri KW. NIH Image to ImageJ: 25 years of image analysis. Nature Methods. 2012;9(7):671–5.

26.Li T, Fan J, Wang B, Traugh N, Chen Q, Liu JS, et al. TIMER: A Web Server for Comprehensive Analysis of Tumor-Infiltrating Immune Cells. Cancer research. 2017;77(21):e108-e10.

27.Bailey MH, Tokheim C, Porta-Pardo E, Sengupta S, Bertrand D, Weerasinghe A, et al. Comprehensive Characterization of Cancer Driver Genes and Mutations. Cell. 2018;173(2):371–85.e18.

28.Belinky F, Nativ N, Stelzer G, Zimmerman S, Iny Stein T, Safran M, et al. PathCards: multi-source consolidation of human biological pathways. Database. 2015;2015.

29.Xiao A, Cheng Z, Kong L, Zhu Z, Lin S, Gao G, et al. CasOT: a genome-wide Cas9/gRNA off-target searching tool. Bioinformatics (Oxford, England). 2014;30(8):1180–2.

30.Shalem O, Sanjana NE, Zhang F. High-throughput functional genomics using CRISPR–Cas9. Nature Reviews Genetics. 2015;16:299.

31.Ran FA, Cong L, Yan WX, Scott DA, Gootenberg JS, Kriz AJ, et al. In vivo genome editing using Staphylococcus aureus Cas9. Nature. 2015;520:186.

32.Haeussler M, Schönig K, Eckert H, Eschstruth A, Mianné J, Renaud J-B, et al. Evaluation of off-target and on-target scoring algorithms and integration into the guide RNA selection tool CRISPOR. Genome Biology. 2016;17(1):148.

33.Xu H, Xiao T, Chen CH, Li W, Meyer CA, Wu Q, et al. Sequence determinants of improved CRISPR sgRNA design. Genome research. 2015;25(8):1147–57.

34.Cancer Genome Atlas N. Comprehensive molecular portraits of human breast tumours. Nature. 2012;490(7418):61–70.

35.Cancer Genome Atlas Research N, Weinstein JN, Collisson EA, Mills GB, Shaw KRM, Ozenberger BA, et al. The Cancer Genome Atlas Pan-Cancer analysis project. Nat Genet. 2013;45(10):1113–20.

36.Mounir M, Lucchetta M, Silva TC, Olsen C, Bontempi G, Chen X, et al. New functionalities in the TCGAbiolinks package for the study and integration of cancer data from GDC and GTEx. PLoS computational biology. 2019;15(3):e1006701.

37.Mi H, Muruganujan A, Ebert D, Huang X, Thomas PD. PANTHER version 14: more genomes, a new PANTHER GO-slim and improvements in enrichment analysis tools. Nucleic Acids Res. 2018;47(D1):D419-D26.

38.Jagarlamudi KK, Shaw M. Thymidine kinase 1 as a tumor biomarker: technical advances offer new potential to an old biomarker. Biomarkers in Medicine. 2018;12(9):1035–48.

39.Haveman J, Sigmond J, van Bree C, Franken NA, Koedooder C, Peters GJ. Time course of enhanced activity of deoxycytidine kinase and thymidine kinase 1 and 2 in cultured human squamous lung carcinoma cells, SW–1573, induced by gamma-irradiation. Oncology reports. 2006;16(4):901–5.

40.Seyfried TN, Huysentruyt LC. On the origin of cancer metastasis. Crit Rev Oncog. 2013;18(1–2):43–73.

41.Zhu X, Shi C, Peng Y, Yin L, Tu M, Chen Q, et al. Thymidine kinase 1 silencing retards proliferative activity of pancreatic cancer cell via E2F1-TK1-P21 axis. Cell Prolif. 2018;51(3):e12428.

42.O'Neill KL, Zhang F, Li H, Fuja DG, Murray BK. Thymidine kinase 1—A prognostic and diagnostic indicator in ALL and AML patients. Leukemia. 2007;21(3):560–3.

43.Zheng B, Fiumara P, Li YV, Georgakis G, Snell V, Younes M, et al. MEK/ERK pathway is aberrantly active in Hodgkin disease: a signaling pathway shared by CD30, CD40, and RANK that regulates cell proliferation and survival. Blood. 2003;102(3):1019–27.

44.Flusberg DA, Sorger PK. Surviving apoptosis: life-death signaling in single cells. Trends Cell Biol. 2015;25(8):446–58.

45.Li Y, Barbash O, Diehl JA. 11 - Regulation of the Cell Cycle. In: Mendelsohn J, Gray JW, Howley PM, Israel MA, Thompson CB, editors. The Molecular Basis of Cancer (Fourth Edition). Philadelphia: Content Repository Only!; 2015. p. 165–78.e2.

46.Barbash O, Alan Diehl J. Chapter 13 - Regulation of the Cell Cycle. In: Mendelsohn J, Howley PM, Israel MA, Gray JW, Thompson CB, editors. The Molecular Basis of Cancer (Third Edition). Philadelphia: W. B. Saunders; 2008. p. 177–88.

47.Cui Y, Riedlinger G, Miyoshi K, Tang W, Li C, Deng C-X, et al. Inactivation of Stat5 in mouse mammary epithelium during pregnancy reveals distinct functions in cell proliferation, survival, and differentiation. Molecular and cellular biology. 2004;24(18):8037–47.

48.Lawlor MA, Alessi DR. PKB/Akt: a key mediator of cell proliferation, survival and insulin responses? Journal of cell science. 2001;114(Pt 16):2903–10.

49.Meloche S, Pouyssegur J. The ERK1/2 mitogen-activated protein kinase pathway as a master regulator of the G1- to S-phase transition. Oncogene. 2007;26(22):3227–39.

50.Yu JSL, Cui W. Proliferation, survival and metabolism: the role of PI3K/AKT/mTOR signalling in pluripotency and cell fate determination. Development. 2016;143(17):3050.

51.Wu F, Zhou L, Jin W, Yang W, Wang Y, Yan B, et al. Anti-Proliferative and Apoptosis-Inducing Effect of Theabrownin against Non-small Cell Lung Adenocarcinoma A549 Cells. Front Pharmacol. 2016;7:465-.

52.An S, Zheng Y, Bleu T. Sphingosine 1-phosphate-induced cell proliferation, survival, and related signaling events mediated by G protein-coupled receptors Edg3 and Edg5. The Journal of biological chemistry. 2000;275(1):288–96.

53.Zhang Y, Hunter T. Roles of Chk1 in cell biology and cancer therapy. International journal of cancer. 2014;134(5):1013–23.

Tables

Table 1: Correlations between TK1 and invasive factors in BRCA RNA-seq patient data

Negative Correlations								
Protein	**Correlation**	**P value**	**Protein**	**Correlation**	**P value**	**Protein**	**Correlation**	**P value**
ETS2	-0.176	4.43E-09	MMP10	-0.099	9.75E-04	VIM	-0.074	1.44E-02
JUN	-0.105	4.84E-04	MMP16	-0.368	0.00E+00	CTNNB1	-0.275	2.28E-20
TIMP2	-0.208	3.60E-12	MMP17	-0.075	1.24E-02	MMP23	-0.201	1.76E-11
TIMP3	-0.257	5.46E-18	MMP19	-0.141	2.70E-06	MMP2	-0.234	4.80E-15
TIMP4	-0.263	8.04E-19	ETS1	-0.208	4.07E-12	MMP3	-0.099	1.06E-03
SNAI2	-0.246	1.80E-16	PRKB	-0.098	1.21E-03	LAMC1	-0.246	1.60E-16
GSC	-0.108	3.41E-04	PIK3CA	-0.202	1.54E-11	Zeb2	-0.336	0
FoxC2	-0.153	3.42E-07	Twist1	-0.105	4.93E-04	NFKB1	-0.330	0
			Twist2	-0.139	3.65E-06			
Positive Correlations								
Protein	**Correlation**	**P value**	**Protein**	**Correlation**	**P value**	**Protein**	**Correlation**	**P value**
ApoE	0.204	8.69E-12	TCF3	0.220	2.07E-13	MMP8	0.114	1.51E-04
ITGB2	0.092	2.32E-03	CDH1	0.090	2.77E-03	MMP9	0.220	2.11E-13
ITGB7	0.202	1.47E-11	CTSD	0.106	4.50E-04	MMP12	0.226	3.14E-14
CD24	0.062	4.06E-02	CTSB	0.115	1.38E-04	MMP15	0.197	4.78E-11
F11R	0.220	2.06E-13	PLAU	0.066	2.90E-02	BSG	0.319	0.00E+00
Snai1	0.195	6.88E-11	MMP1	0.303	8.99E-25	TNF	0.149	6.61E-07

Table 2: Correlations between TK1 and apoptotic factors in BRCA RNA-seq patient data

Negative Correlations							
Protein	Correlation	Protein	Correlation	Protein	Correlation	Protein	Correlation
RPS6KA2	-0.434	INSR	-0.292	FLT1	-0.246	CAPN5	-0.153
TGFBR2	-0.433	NTRK3	-0.292	FGFR1	-0.245	MTOR	-0.153
ATM	-0.414	GABRA2	-0.290	ITGA4	-0.228	ITGB1	-0.151
BCL2	-0.409	MAPK8	-0.203	RNMT	-0.223	BMPR1A	-0.147
ERBB4	-0.397	IKBKB	-0.288	RPS6KA6	-0.221	CAPN3	-0.143
TP53BP1	-0.396	AKT3	-0.287	PIK3R4	-0.215	CHUK	-0.135
PIK3C2A	-0.395	TGFBR3	-0.286	GABRB2	-0.215	CAPN6	-0.133
NTRK2	-0.389	CTNNB1	-0.275	BMPR1B	-0.213	EGFR	-0.131
ITGAV	-0.370	CAPN11	-0.271	GABRG1	-0.210	FGFR2	-0.130
CAPN8	-0.368	PPP2CB	-0.261	TGFBR1	-0.203	MAPK9	-0.130
PDPK1	-0.362	CAPN7	-0.261	PIK3CA	-0.202	IL5RA	-0.127
ACVR1	-0.352	CAPN13	-0.256	FLT4	-0.195	ATR	-0.123
PRKCE	-0.346	RPS6KA3	-0.255	GABRA4	-0.195	ITGA11	-0.119
PIK3C3	-0.335	IL1R1	-0.255	SLTM	-0.194	KRAS	-0.119
NFKB1	-0.330	ACVR1B	-0.255	MDM2	-0.193	MAPK10	-0.106
PIK3R1	-0.330	ERBB3	-0.254	PRKCA	-0.191	JUN	-0.105
IGF1R	-0.327	PRKCH	-0.250	CAPN9	-0.190	MAPK14	-0.098
PDGFRB	-0.317	NGFR	-0.250	GABRB3	-0.179	PRKCB	-0.098
KDR	-0.308	ANTXR1	-0.248	CASP9	-0.177	PPP2CA	-0.092
PDGFRA	-0.302	PIK3C2B	-0.248	PIK3C2G	-0.172	CASP10	-0.085
CASP12	-0.298	PIK3CG	-0.247	IGF2R	-0.154	NTRK1	-0.084
ERBB2	-0.060	NOS3	-0.065	PIK3CD	-0.082	GABRB1	-0.084
PIK3R5	-0.060	MET	-0.062	CAPN2	-0.069		
Positive Correlations							
Protein	Correlation	Protein	Correlation	Protein	Correlation	Protein	Correlation
IL1A	0.060	AKT1	0.111	GABRQ	0.169	IKBKG	0.221
GABRD	0.066	IL1R2	0.120	CAPN1	0.171	MAP2K2	0.285
GABRE	0.066	PRKCG	0.127	GABRA3	0.179	YWHAZ	0.308
PTK2	0.067	CAPN10	0.129	CAPN12	0.183	GSK3A	0.322
MAP2K1	0.074	IL2RA	0.139	CASP3	0.191	BAX	0.346
IL13	0.079	MAPK12	0.140	YWHAG	0.199	HRAS	0.353
YWHAE	0.104	FGFR4	0.140	MMAB	0.203	CSNK2B	0.476
PRKCZ	0.109	RELA	0.156	YWHAH	0.206	CHEK2	0.535
		MAPK13	0.159	NFKB2	0.213	CHEK1	0.574
		CSNK2A2	0.165	YWHAQ	0.216		

Table 3: Correlations between TK1 and cell cycle checkpoint factors in BRCA RNA-seq patient data

Negative Correlations

Protein	Correlation	Protein	Correlation	Protein	Correlation	Protein	Correlation
AM175A	-0.482	WRN	-0.227	PSMD5	-0.121	HIST2H2BE	-0.081
ATM	-0.414	CDKN1B	-0.225	CDC27	-0.110	CDC16	-0.079
P53BP1	-0.396	MDM4	-0.223	ANAPC1	-0.094	RNF168	-0.075
RAD50	-0.337	ANAPC4	-0.219	ORC2l	-0.093	MRE11A	-0.074
RAD17	-0.319	MDM2	-0.193	ZNF385A	-0.092	ATRIP	-0.067
HERC2	-0.311	HIST4H4	-0.147	WEE1	-0.091	RBBP8	-0.064
ERCC4	-0.263	RRAD	-0.134	RNASE6	-0.090	ANTXR1	-0.248
		ATR	-0.123	CDKN1A	-0.086		

Positive Correlations

Protein	Correlation	Protein	Correlation	Protein	Correlation	Protein	Correlation
BUB3	0.071	HIST1H4I	0.199	BRIP1	0.330	BLM	0.499
RPA1	0.074	MMAB	0.203	ANAPC7	0.334	MRPL36	0.508
ANAPC10	0.075	PSMD10	0.204	PSMA6	0.350	PSMC3	0.524
RMI1	0.076	YWHAH	0.206	PSME2	0.361	PSMC4	0.527
HIST1H4J	0.079	HIST1H2BM	0.210	PSMD13	0.361	CHEK2	0.535
REXO2	0.083	UBE2N	0.213	PSMB1	0.362	BUB1B	0.546
PIAS4	0.088	YWHAQ	0.216	RFC5	0.362	MCM6	0.551
ORC5l	0.092	BRCA1	0.230	RPA3	0.363	ANAPC11	0.555
PSMC6	0.095	PSMB8	0.230	SFN	0.363	PSMA7	0.557
CDC26	0.095	PSMD1	0.230	RFC3	0.383	MCM5	0.559
YWHAE	0.104	PSME4	0.232	CLSPN	0.389	MCM3	0.567
PSME3	0.104	HIST1H2BH	0.243	C19orf62	0.390	CHEK1	0.574
IST1H2BG	0.105	HIST1H2BE	0.244	PSMA3	0.394	MAD2L1	0.576
IST1H2BF	0.106	WHSC1	0.247	PSMD3	0.395	DEPDC1B	0.577
HIST2H4A	0.112	PSMB9	0.248	PSMC1	0.401	CCNE1	0.578
HIST1H4F	0.114	PCBP4	0.249	PSMC5	0.405	MCM7	0.591
UBE2E1	0.122	MCM8	0.250	CDK2	0.409	RFC4	0.595
HIST1H4D	0.128	PSMB10	0.254	DNA2	0.410	ORC1l	0.609
RPS27A	0.130	UBB	0.257	C12orf32	0.410	CCNA2	0.612
ARTN	0.132	cdkn2a	0.259	PSMB6	0.412	C16orf75	0.613
PSMD6	0.134	SUMO1	0.261	PSMD7	0.412	GTSE1	0.620
HIST1H4H	0.138	HIST1H4C	0.268	PSMD4	0.419	MCM2	0.621
RAD9B	0.142	HIST1H4B	0.270	PSMD8	0.424	CDC6	0.622
RFWD2	0.147	HIST1H2BK	0.275	MCM4	0.425	CDK1	0.623
PSMF1	0.151	UBA52	0.275	PSMC2	0.425	EXO1	0.628
HIST1H2BN	0.152	RAD9A	0.275	PSMD12	0.430	MCM10	0.629
RAD1	0.153	RNF8	0.281	PSMB7	0.436	CDC25C	0.635
HIST1H2BB	0.153	HIST1H2BL	0.285	PSMA5	0.437	ORC6l	0.635
PSME1	0.158	MAD1L1	0.291	PSMD2	0.439	CDC25A	0.638
HIST1H4E	0.164	HIST1H4A	0.302	PSMB3	0.444	CCNB1	0.642
ANAPC5	0.167	YWHAZ	0.308	PSMD14	0.454	RFC2	0.649
MDC1	0.170	PSMA1	0.314	PSMA4	0.455	H2AFX	0.652
HIST1H4L	0.172	HIST1H2BJ	0.315	CCNE2	0.468	CCNB2	0.675
UBC	0.189	PSMD9	0.315	PSMB4	0.473	CDC20	0.696
TOPBP1	0.190	HIST1H2BO	0.317	DBF4	0.474	CDC45	0.706
HIST1H2BI	0.193	PSMA2	0.317	PSMB2	0.483	UBE2C	0.706
YWHAG	0.199	UBE2V2	0.323	CDC7	0.486	PKMYT1	0.734
		PSMD11	0.330	PSMB5	0.488		

Figures

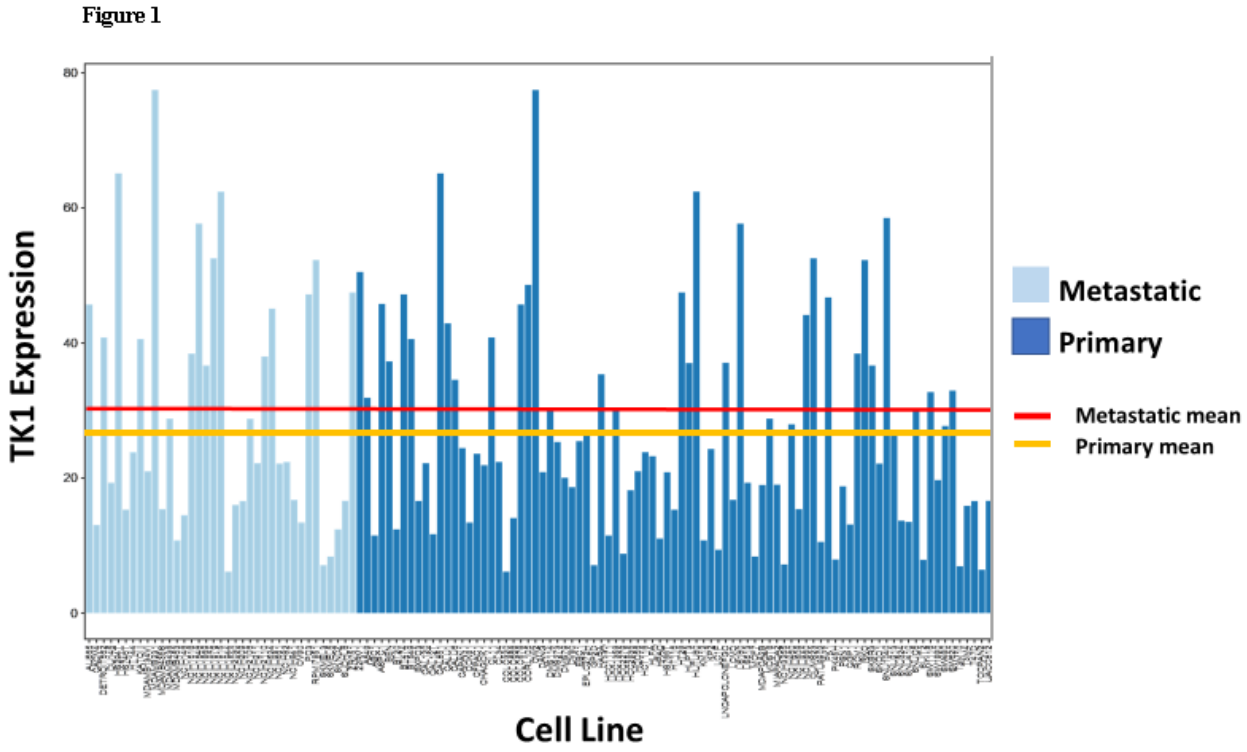

Figure 1

Comparing TK1 levels in metastatic and primary cancer cell lines

Figure 2:

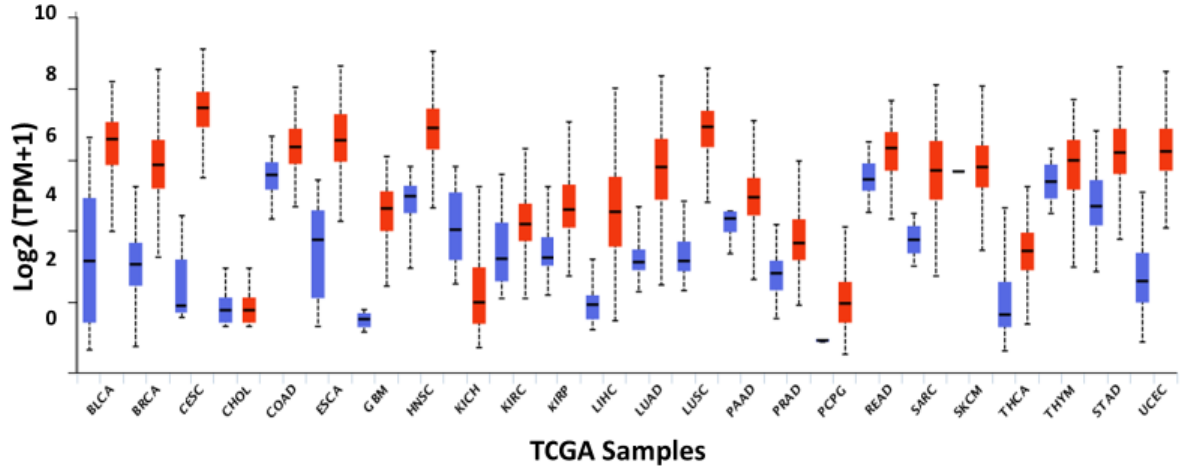

Figure 2

Expression of TK1 across TCGA cancers

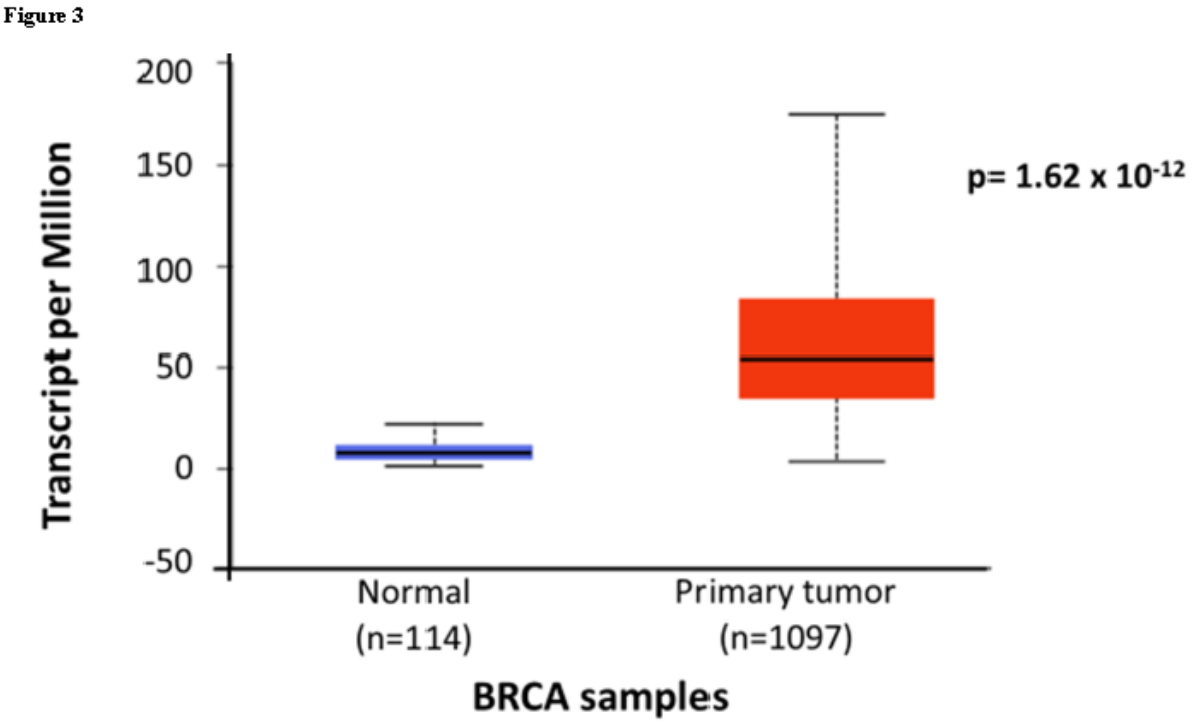

Figure 3

TK1 levels in normal breast tissue and primary BRCA tumor

Figure 4

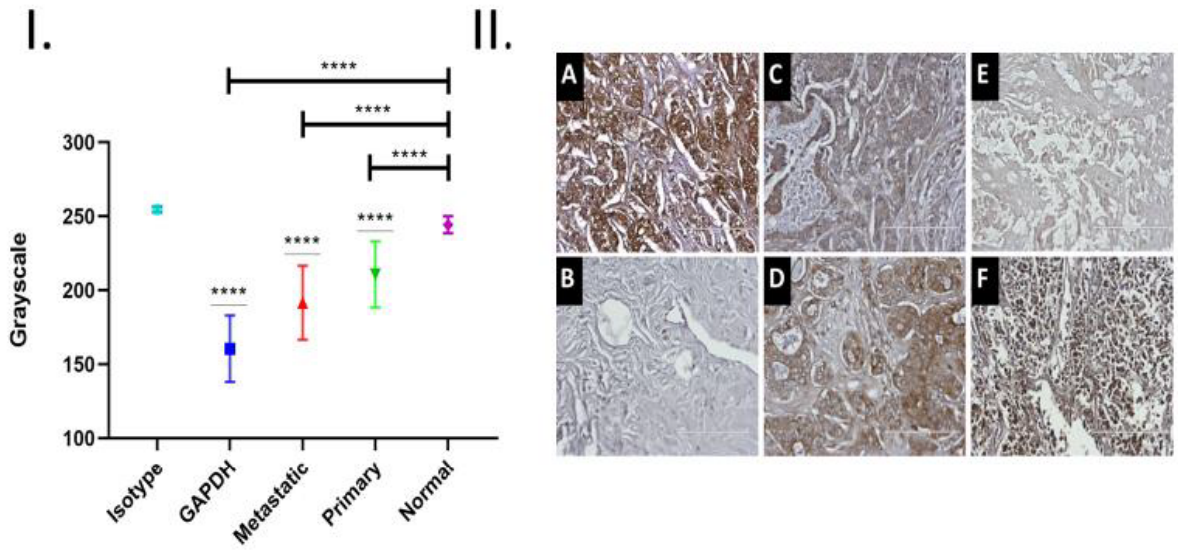

Figure 4

Immunohistochemistry staining of TK1 in invasive ductal and infiltrating lobular with matched metastatic and adjacent normal samples.

Figure 5

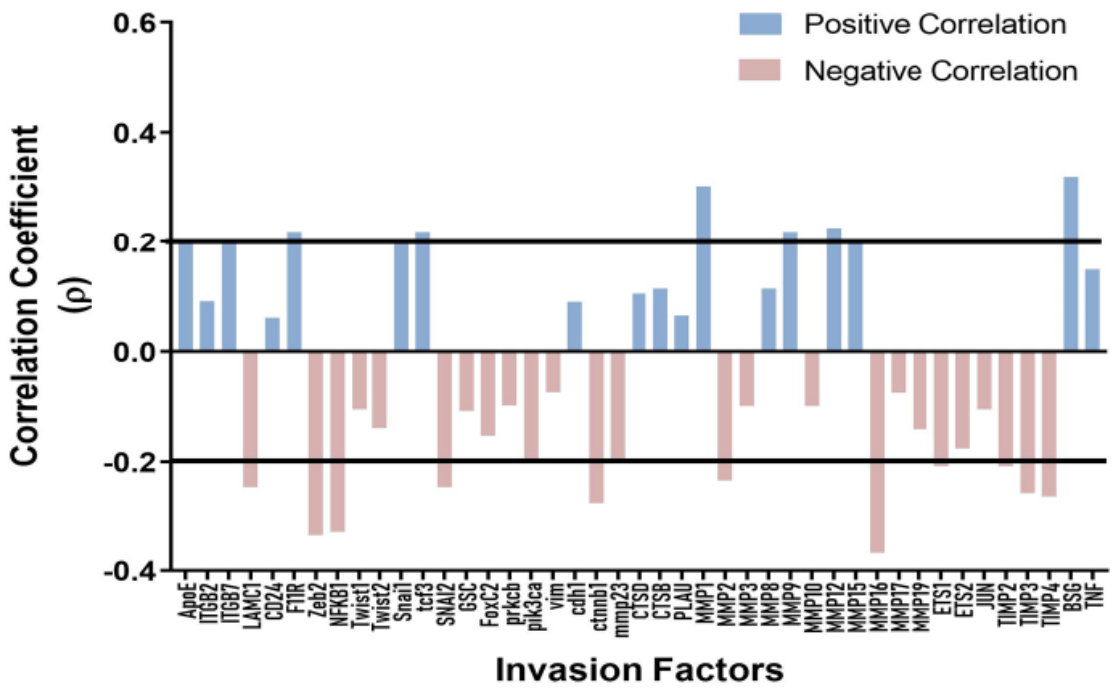

Figure 5

Visual depiction of correlation strength between TK1 and invasive factors

Figure 6

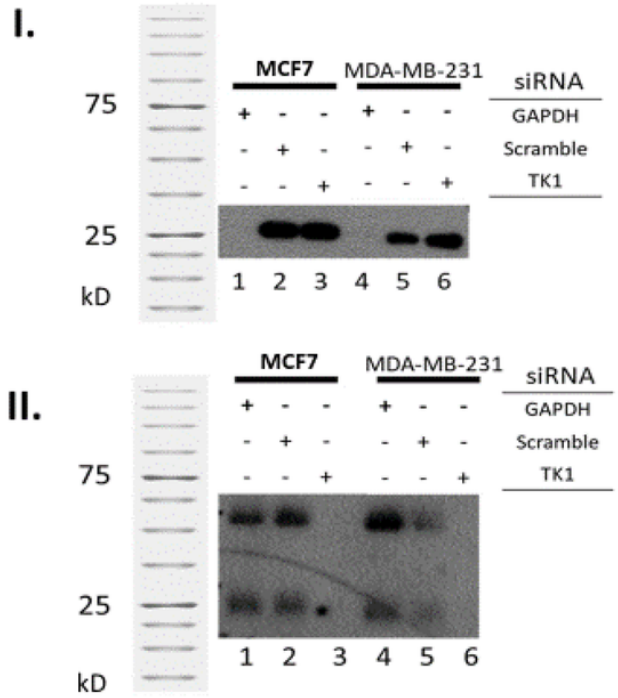

Figure 6

Confirming TK1-/- in siRNA treated cell lines MDA-MB-231 and MCF7

Figure 7

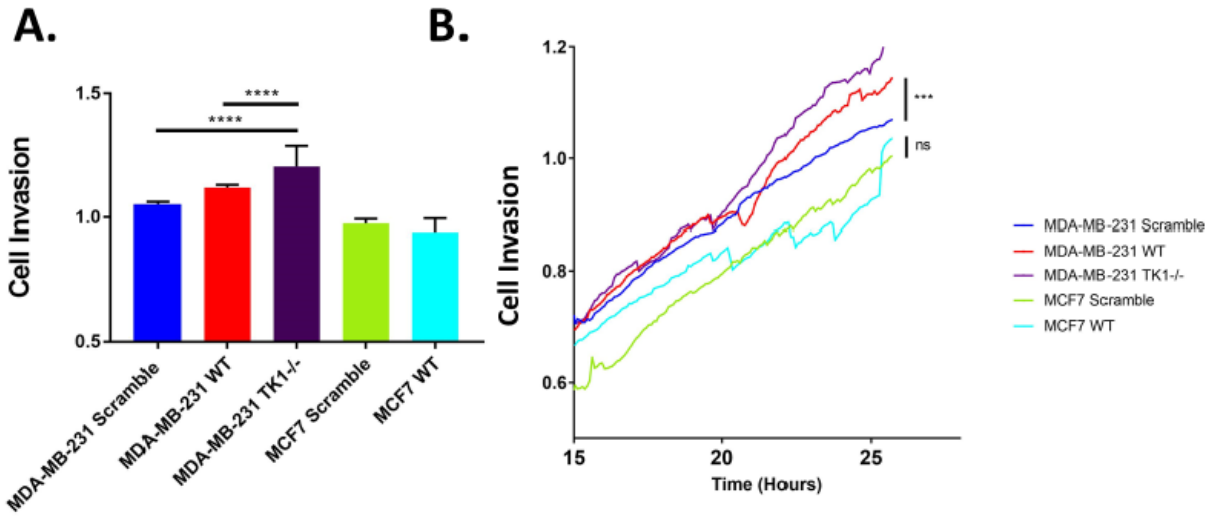

Figure 7

Cellular invasion assay comparing MDA-MB-231 wild type and TK1-/- cells

Figure 8

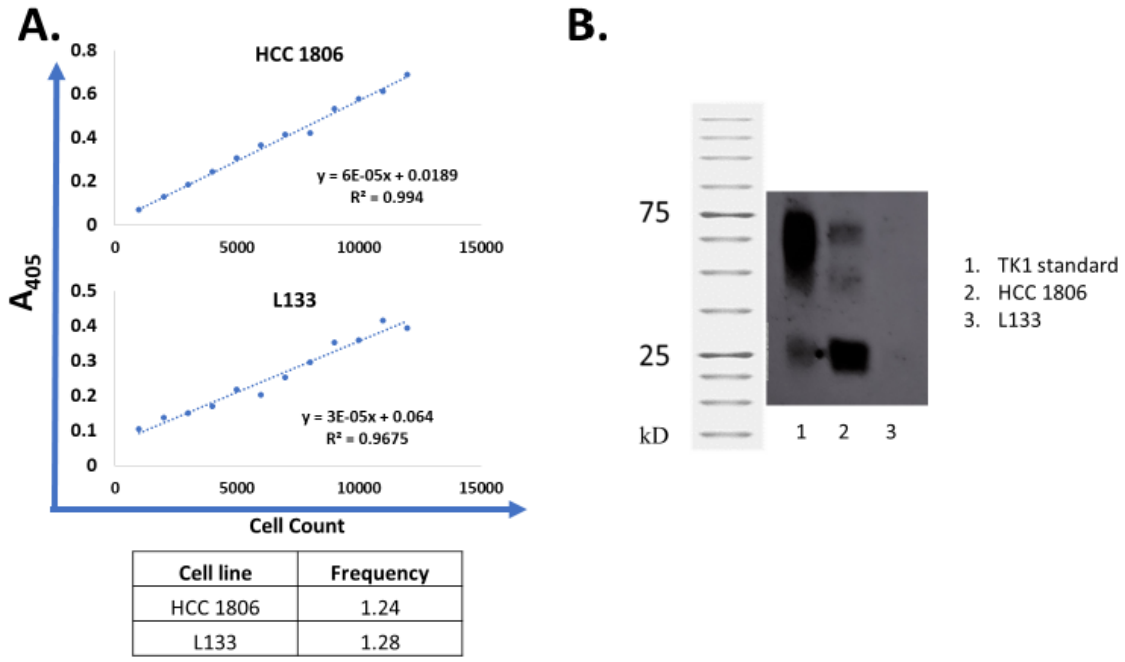

Cell line	Frequency
HCC 1806	1.24
L133	1.28

Figure 8

CRISPR-Cas9 HCC 1806 TK1-/- western blot and nitrophenyl phosphate cell proliferation assay testing doubling time in 24 hours (frequency) for HCC 1806 and L133TK1-/- cells

Figure 9

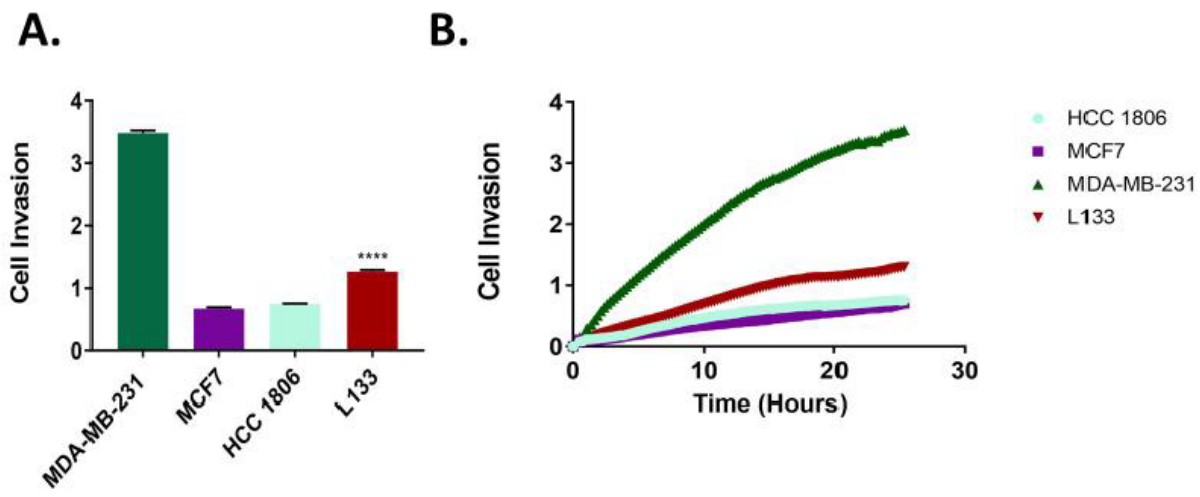

Figure 9

Cellular invasion analysis comparing HCC 1806 and L133TK1-/- cell lines

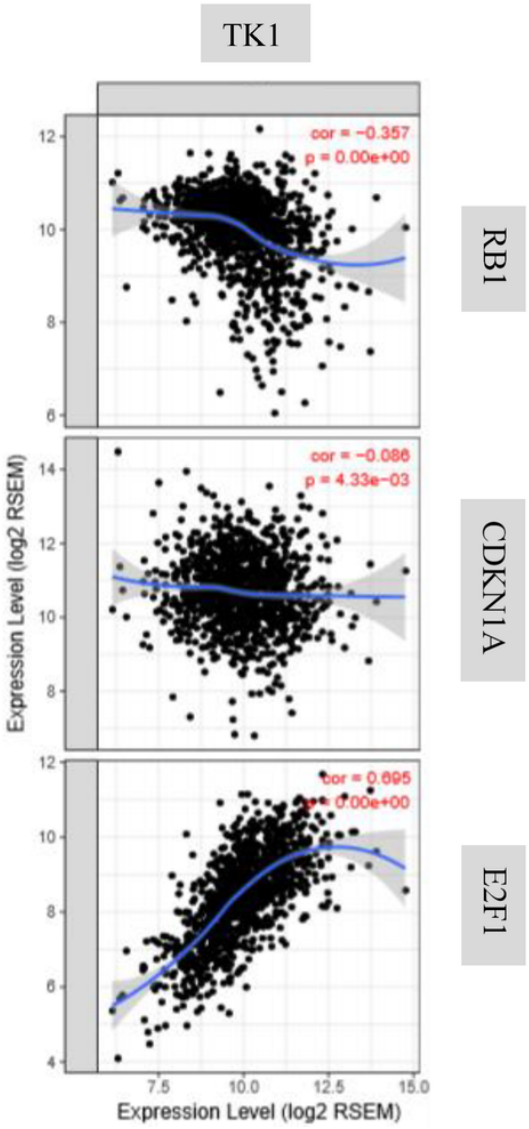

Figure 10

Figure 10

Correlation plots of TK1 vs. RB1, CDKN1A, and E2F1 in BRCA patients

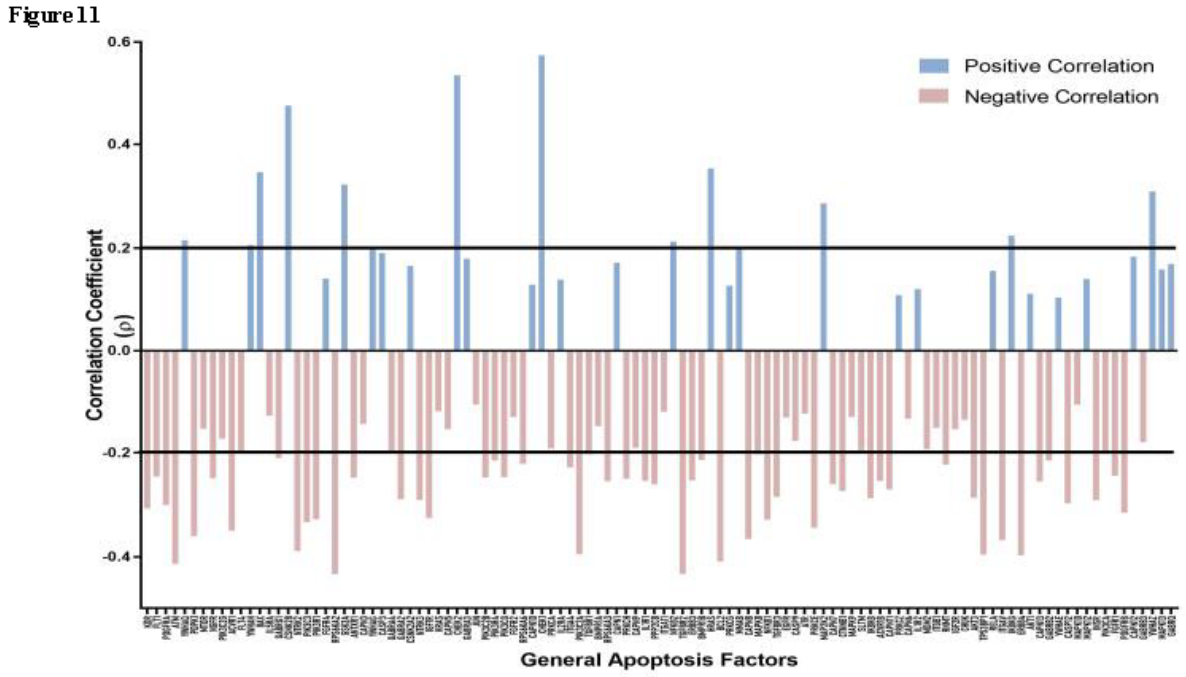

Figure 11

Visual depiction of correlation strength and between TK1 and apoptotic factors

Figure 12

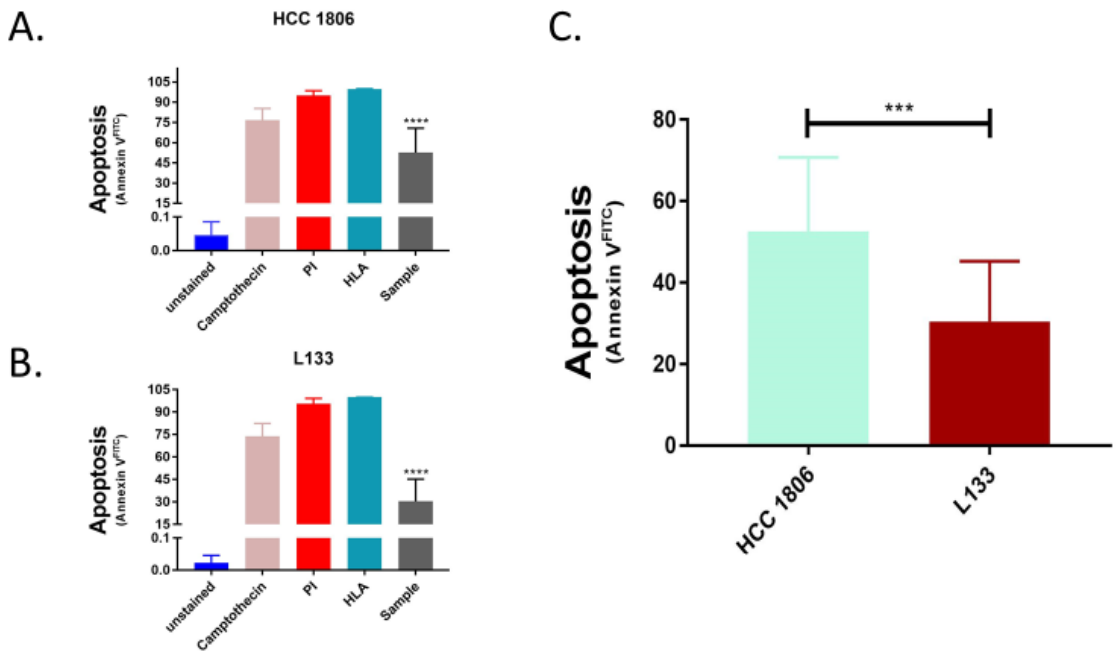

Figure 12

Annexin V results testing glucose deprived and hypoxic induced apoptosis in HCC 1806 and L133TK1-/- cell lines

Figure 13

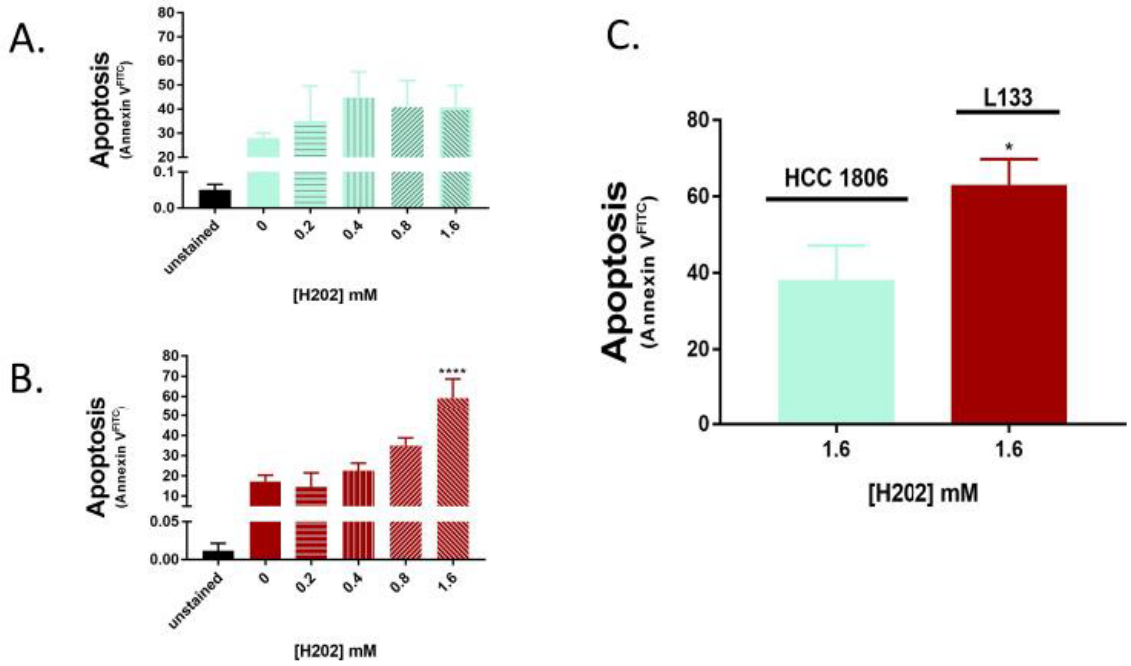

Figure 13

Annexin V results from oxidative induced apoptosis using hydrogen peroxide in HCC 1806 and L133TK1-/- cell lines

Figure 14

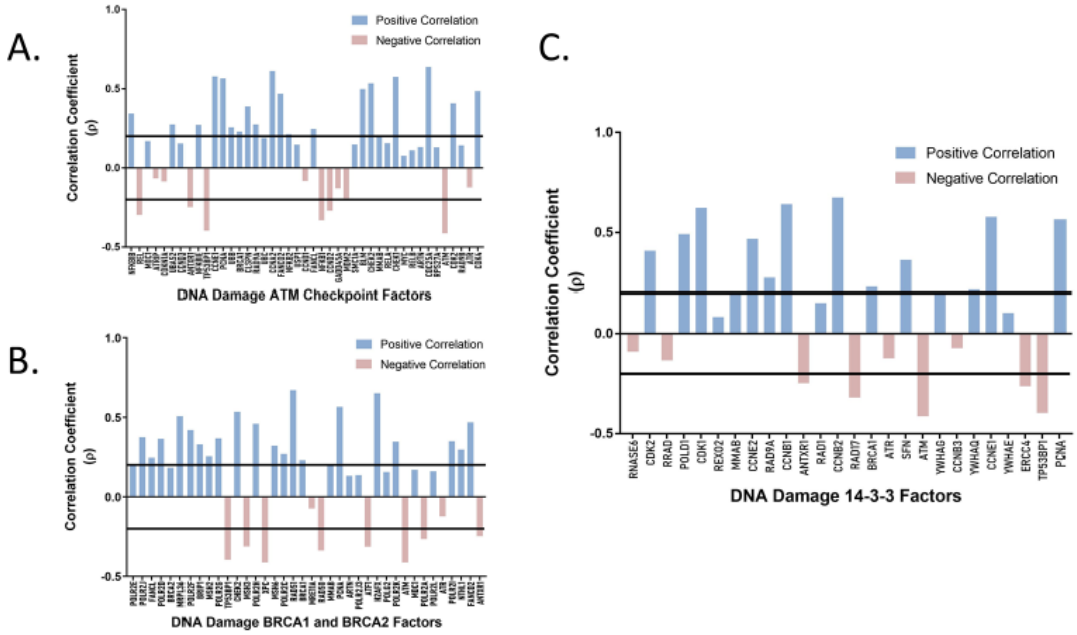

Figure 14

Visual depiction of correlation strength between TK1 and different DNA damage pathways

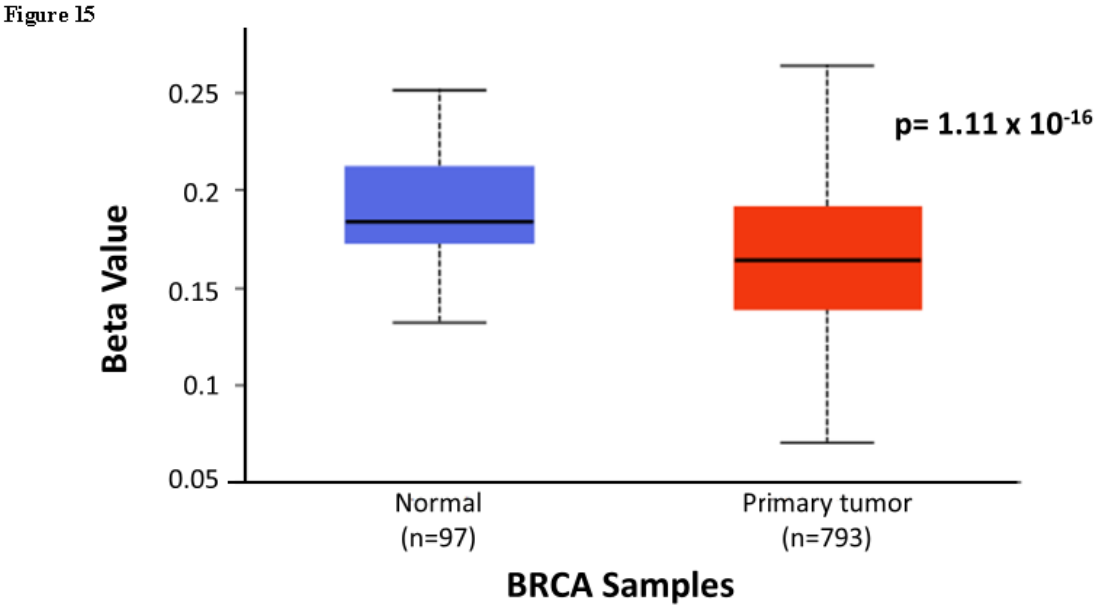

Figure 15

Comparing methylation at the TK1 promoter between normal tissue and primary tumor samples

Figure 16

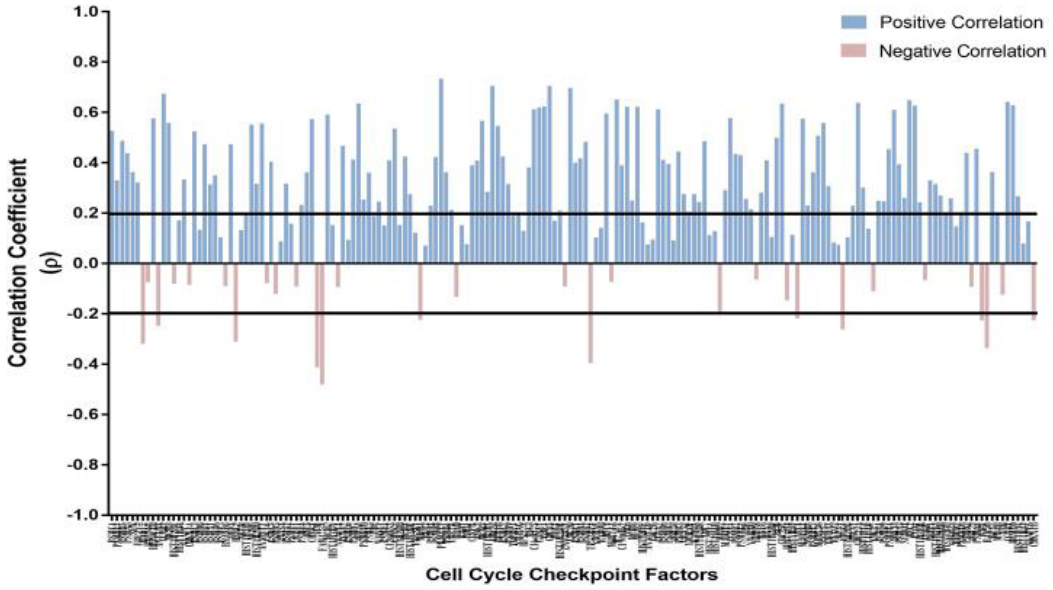

Figure 16

Visual depiction of correlation strength between TK1 and Cell Cycle Checkpoint Factors

Figure 17

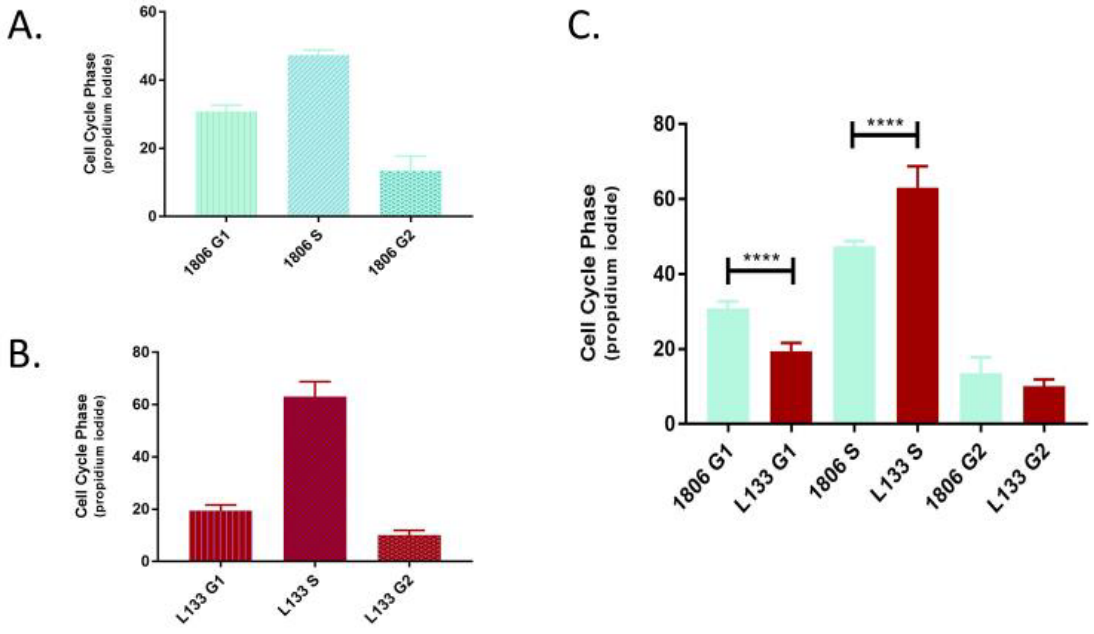

Figure 17

Cell cycle results analyzing cell populations in G1, S and G2 between HCC 1806 and L133TK1-/- cells Flow cytometry results of cell cycle analysis measuring propidium iodide staining. A. Comparing means of HCC 1806 controls and samples. B. Comparing means of L133TK1-/- controls and samples. C. CRISPR-Cas9 treated cell line L133TK1-/- has increased apoptosis when compared to HCC 1806 cell line.

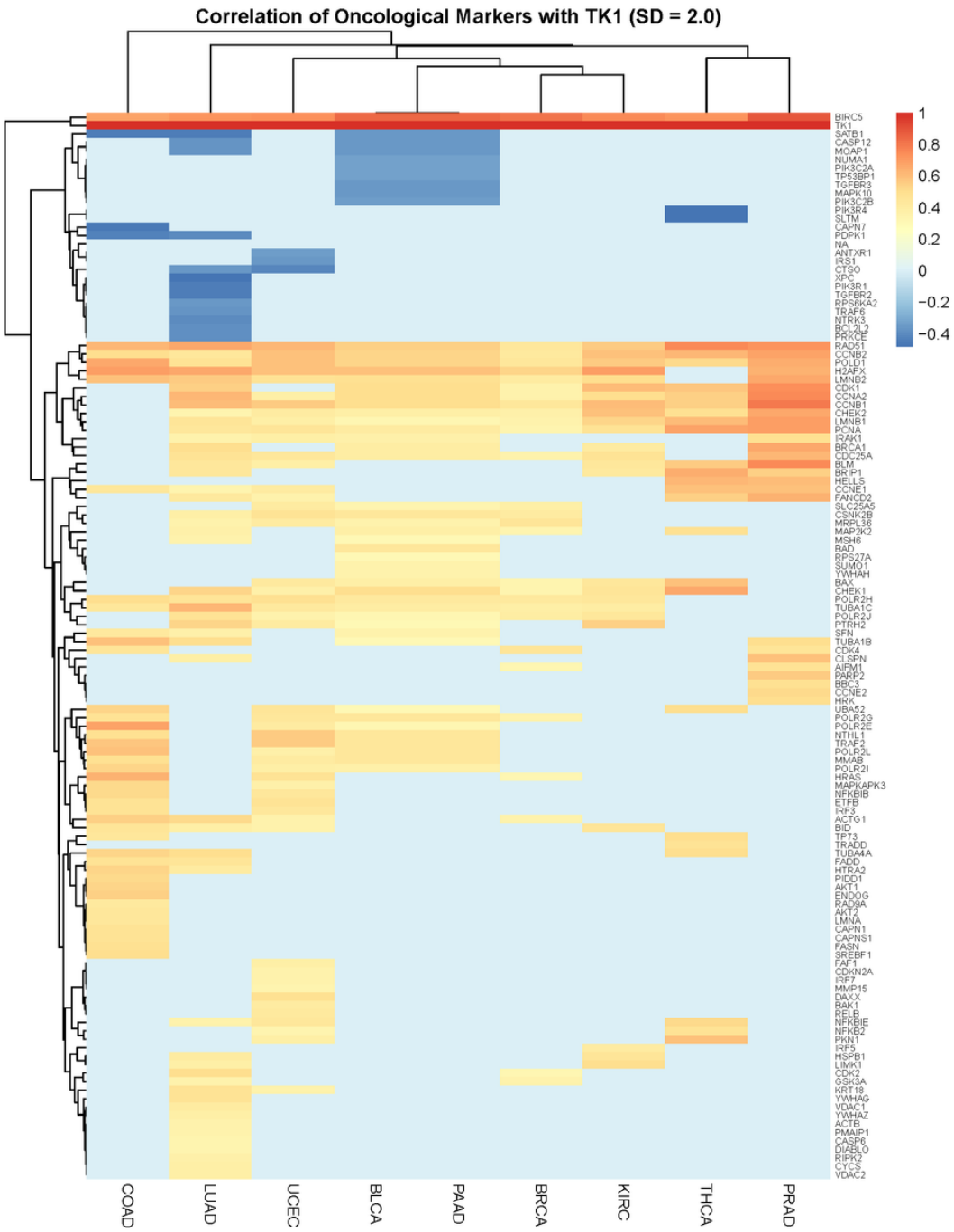

Figure 18

Heatmap of TK1 correlations to invasive, apoptotic and cancer promoting genes across nine different TCGA cancers

Supplementary Files

This is a list of supplementary files associated with this preprint. Click to download.

- AdditionalFile3.csv
- AdditionalFile4.pdf
- AdditionalFile2.pdf
- Methodsformula.docx

- AdditionalFile1.pdf